Organic & Biomolecular Chemistry

ROYAL SOCIETY OF CHEMISTRY

REVIEW

View Article Online
View Journal | View Issue

Cite this: *Org. Biomol. Chem.*, 2025, **23**, 7501

Recent advances in the synthesis of multiple helicenes

Zhen Chen,[a,b] Wei-Chen Guo[a,b] and Chuan-Feng Chen *[a,b]

Multiple helicenes, as helically twisted polycyclic frameworks with extended π-conjugated systems, have attracted growing attention due to their unique topologies, tunable chiroptical properties, and potential applications in chiral materials and organic electronics. In this review, we provide a systematic overview of the recent advances in the field of multiple helicenes and propose a concise classification strategy that classifies them into linear, cyclic, and cross-linked types. Based on this classification, we further summarize and highlight a range of efficient synthetic strategies that facilitate the construction of multiple helicenes. We hope this review will provide the design inspiration of multiple helicenes and further be helpful for the development of helicene chemistry.

Received 12th June 2025,
Accepted 17th July 2025

DOI: 10.1039/d5ob00966a

rsc.li/obc

1 Introduction

Helicenes are a class of compounds characterized by their unique twisted stereo helical structures, formed by *ortho*-fused aromatic or heteroaromatic rings.[1–4] This unique chirality, structural variety, and optical/electronic properties endow helicenes with remarkable physicochemical properties, making them highly attractive for applications in various fields, including asymmetric catalysis, chiral recognition, and chiral optical materials.[5–11]

Depending on the number of helical units present in the molecule, helicenes can be broadly classified into two categories: single helicenes containing one helical unit and multiple helicenes incorporating two or more helical units within a single molecule. Compared to single helicenes, multiple helicenes exhibit more distinctive properties. First, multiple helicenes possess more complex stereo-structures, owing to the incorporation of multiple helical units within a single molecule. The spatial orientation and connectivity of these helical structures can vary significantly, giving rise to a wide range of molecular topologies. This structural diversity introduces new dimensions to stereochemistry and conformational control, far beyond what is achievable with single helicenes. Second, the presence of multiple helical units in one molecule results in multi-chirality, where each helical unit can independently adopt a P or M configuration. This gives rise to a complex set of stereoisomers with distinct chiral properties, including multiple diastereomers and enantiomers. This also leads to

[a]*Beijing National Laboratory for Molecular Sciences, CAS Key Laboratory of Molecular Recognition and Function, Institute of Chemistry, Chinese Academy of Sciences, Beijing 100190, China. E-mail: cchen@iccas.ac.cn*
[b]*University of Chinese Academy of Sciences, Beijing 100049, China*

Zhen Chen

Zhen Chen received his BS degree from the University of Science and Technology of China in 2021 and MS degree from the same University of Science and Technology of China in 2024 under the supervision of Prof. Zhenhua Gu. In 2024, he joined the laboratory of Prof. Chuan-Feng Chen at ICCAS to pursue his PhD degree in chemistry. His research focus is on the design of B,N embedded hetero-helicene TADF materials and their application in CP-OLEDs.

Wei-Chen Guo

Wei-Chen Guo received his BS degree from China University of Petroleum (Beijing). In 2021, he joined the laboratory of Prof. Chuan-Feng Chen at the Institute of Chemistry, Chinese Academy of Sciences, to pursue his PhD degree in chemistry. His research interest is on high-performance circularly polarized electroluminescent materials based on B,N embedded hetero-helicenes.

unique molecular packing, solid state chirality and self-assembly behaviours. Third, multiple helicenes generally feature larger π-conjugated systems than their single helicene counterparts. The extended conjugation facilitates stronger electronic communication throughout the molecule, resulting in unique optical absorption, emission properties, and electronic characteristics. These properties make them promising candidates for applications in optoelectronic materials, molecular electronics, and spintronics.

The synthesis of complex multiple helicenes presents significant challenges due to their inherent strain and the need for precise stereochemical control. To overcome these obstacles, several powerful synthetic strategies have been developed (Fig. 1). Oxidative coupling reactions, particularly Scholl reactions and photocyclization, have proven highly effective for constructing extended π-systems and forming multiple rings simultaneously. Transition metal-catalyzed [2 + 2 + 2] cycloadditions offer an atom-economical route to build helical scaffolds, often with good stereoselectivity. Friedel–Crafts alkylation/acylation provides a versatile method for intramolecular cyclization, enabling the closure of helical units. More recently, intramolecular borylation reactions have emerged as a valuable tool, allowing the formation of strained boron-bridged helical structures that are difficult to access using other approaches. These methods collectively provide a robust toolbox for accessing diverse multiple helicene architectures.

Since the first synthesis of double [5]helicene in 1959,[12] the field of multiple helicenes has witnessed rapid and substantial development. Numerous molecular architectures have been reported,[13–15] encompassing bis-, tris-, tetra-, penta-, and hexahelicenes, with diverse geometric arrangements such as S-shaped, X-shaped, M-shaped, fan-shaped topologies and so on. Despite the rapid expansion and growing structural diversity of multiple helicenes, there remains a lack of a unified and systematic classification method to organize these multiple helicene structures. Furthermore, the synthetic strategies developed for constructing multiple helicenes—although often elegant and efficient—have not been comprehensively summarized in a way that highlights their potential applicability across different helicene structures.

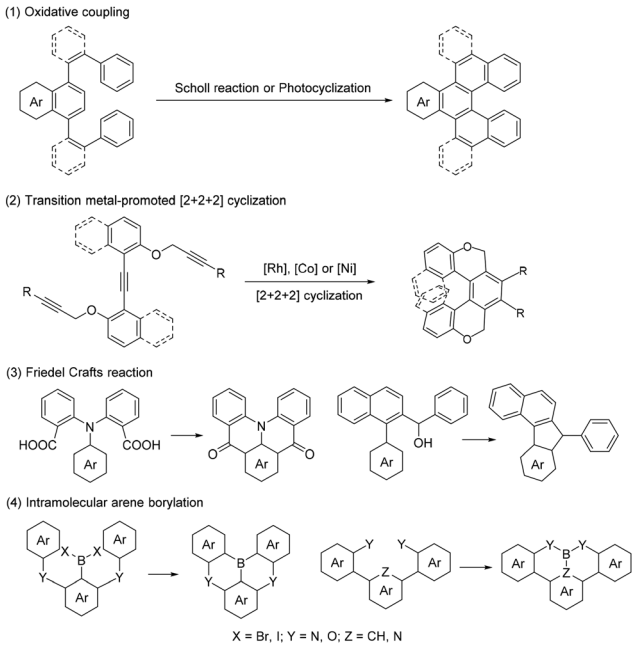

Fig. 1 Several synthetic methods toward multiple helicenes.

In this review, we aim to present a systematic overview of the recent advances in the field of multiple helicenes, and we propose a concise and intuitive classification strategy based on their overall stereostructural characteristics, grouping them into linear, cyclic, and cross-linked categories. This framework not only facilitates a clearer understanding of these complex multiple helicenes but also serves as a guide for future molecular design. Additionally, we summarize and highlight various and efficient synthetic approaches to drive the development, property modification, and application enhancement of multiple helicenes with diverse stereochemical architectures. Through this review, we aim to provide a solid foundation for further exploration and innovation in the field of multiple helicene chemistry, particularly in the development of advanced chiral π-conjugated materials.

Chuan-Feng Chen

Chuan-Feng Chen has been working as a full professor of organic chemistry at the Institute of Chemistry, Chinese Academy of Sciences, since 2001. His current research interests include supramolecular chemistry based on synthetic macrocyclic hosts and organic cages, chiral organic light-emitting materials and helicene chemistry.

2 Linear multiple helicenes

Linearly extended multiple helicene structures are constructed by simplifying each helical unit into a "linear helix," which retains the conjugated backbone while disregarding the three-dimensional helical distortion. These linear helices are then connected *via* aryl cores, such as benzene or naphthalene rings, to form a linearly extended molecular architecture. Analogous to the approach used in higher-order single helicenes, where linear extension is achieved by increasing helicity, in linear multiple helicenes the linear helix is elongated by increasing the number of helicene units.

2.1 Double helicenes

S-shaped double helicenes represent the simplest structural form of linear multiple helicenes, in which each component is fused at the terminal. In recent years, such double helicene compounds have been reported successively. Transition-metal-catalyzed cyclization is a prevalent method for synthesizing helicenes and has recently been used for the synthesis of S-shaped double helicenes. In 2018, Tanaka's group achieved the asymmetric synthesis of an S-shaped double helicene using gold catalysis with (*R*)-BINAP as a chiral phosphine ligand[16] (Fig. 2a). This intramolecular asymmetric hydroarylation yielded the S-shaped double [6]helicene **1** in 29–34% yields and with 64–66% ee.

Besides hydroarylation, [2 + 2 + 2] cycloaddition can also be utilized for synthesizing S-shaped double helicenes. In 2019, Tanaka's group reported a rhodium-catalyzed asymmetric hydroarylation for synthesizing S-shaped double helicenes[17] (Fig. 2b). In the presence of rhodium and the chiral ligand (*R*)-difluorphos, the reaction afforded (−)-**2** and *meso*-**2** S-shaped double [6]helicenes in 45% total yield, with the (−)-**2** isomer exhibiting 73% ee. Both configurations were confirmed by single-crystal X-ray diffraction. Due to steric clashes between the terminal naphthalene rings, the helical chirality of these S-shaped double [6]helicenes is unstable, leading to epimerization between (−)-**2** and *meso*-**2** and eventual racemization at room temperature. In 2020, the same group further reported a highly diastereo- and enantioselective intramolecular double [2 + 2 + 2] cycloaddition catalyzed by a chiral rhodium(I) complex[18] (Fig. 2c). This reaction yielded S-shaped double [6]helicene (−)-**3** with stable helical chirality (>99% ee). The introduction of two additional fused benzene rings significantly enhanced the configurational stability of the helicene. Additionally, Tanaka's group achieved the asymmetric syn-

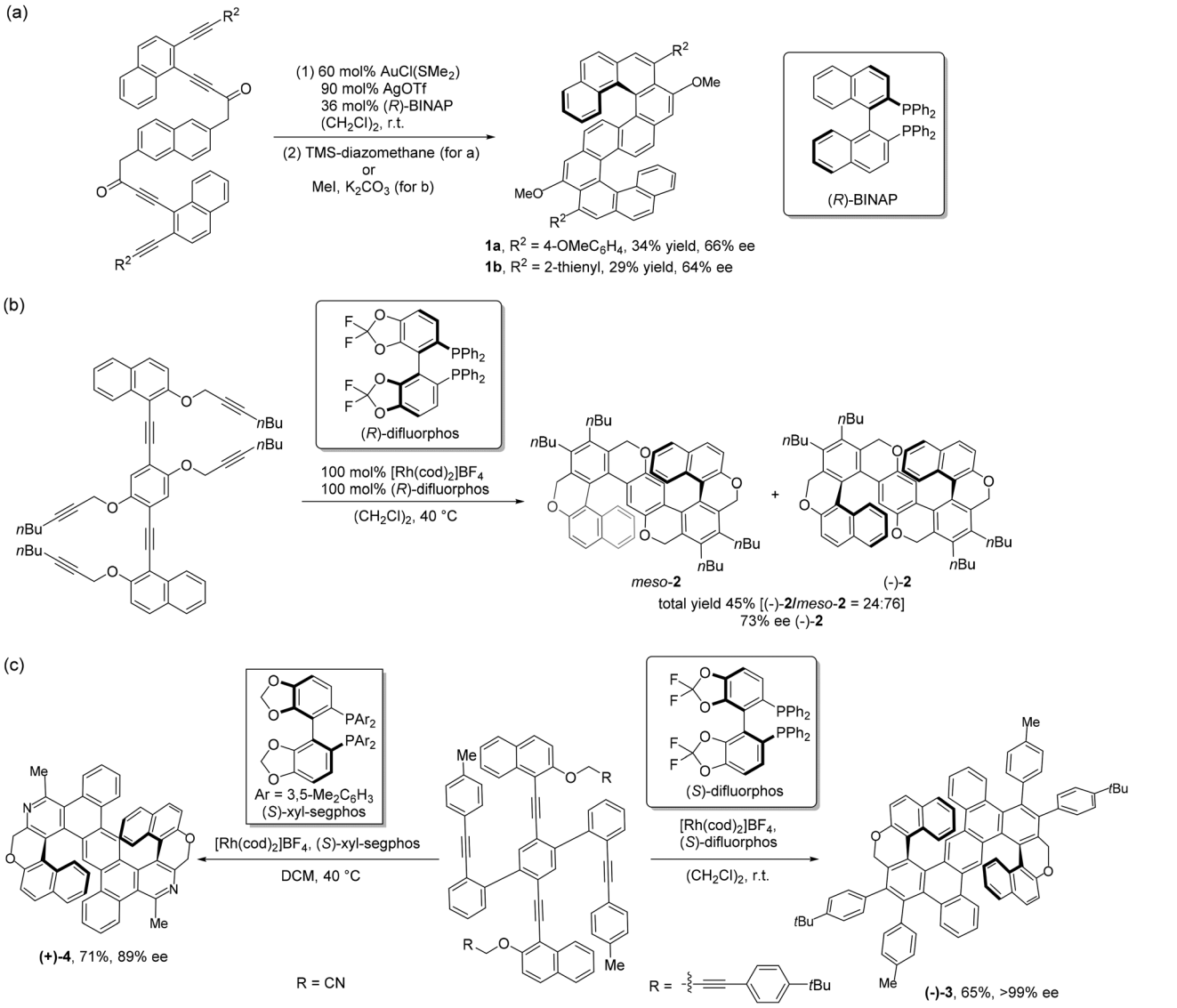

Fig. 2 Transition metal catalyzed synthesis of S-shaped double helicenes.

thesis of nitrogen-incorporated S-shaped double helicenes[19] (Fig. 2c). In 2021, by introducing a cyano group into the substrate, they accomplished the asymmetric synthesis of a pyridine-embedded S-shaped double [6]helicene **4** *via* a cationic rhodium(I)/axially chiral biaryl bisphosphine complex-catalyzed intramolecular [2 + 2 + 2] reaction, affording the target product (+)-**4** in 71% yield with 89% ee.

Friedel–Crafts cyclization is another effective strategy for synthesizing double helicenes. In 2020, Chi's group reported a novel S-shaped double [6]helicene containing two embedded *p*-quinodimethane (*p*-QDM) units[20] (Fig. 3a). By converting an aldehyde-bearing precursor into an alcohol and subsequently inducing Friedel–Crafts cyclization, the double [6]helicene precursor **5a** was synthesized. Subsequent deprotonation with potassium *tert*-butoxide and oxidation with *p*-chloranil yielded the S-shaped double [6]helicene **5b** in 62% yield. This compound exhibited open-shell diradical character, providing insights for designing stable helicenes with diradical properties.

In 2022, Eli Zysman-Colman's group reported their work on the synthesis and properties of a S-shaped [4]double helicene with thermally activated delayed fluorescence[21] (Fig. 3b). The synthesis involved a Cu-catalyzed Ullmann coupling reaction between resorcinol and methyl 2-iodobenzoate, yielding intermediate **6** in 43% yield. Hydrolysis then afforded compound **7** quantitatively, followed by conversion of the carboxylic acid to an acyl chloride and Friedel–Crafts cyclization catalyzed by $AlCl_3$, yielding the S-shaped double [4]helicene **8** in 36% yield.

Similar to S-shaped helicenes, M-shaped helicenes also exhibit a linear molecular structure. In 2022, Yang's research group synthesized a boron–nitrogen–sulfur-doped double [5]helicene with circularly polarized luminescence and thermally activated delayed fluorescence properties[22] (Fig. 4).

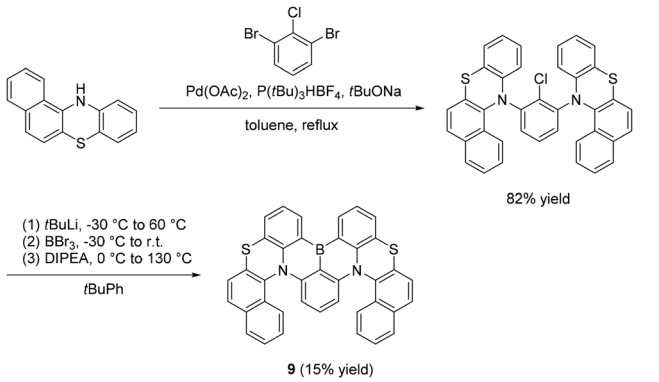

Fig. 4 Synthetic routes to the M-shaped double helicene **9**.

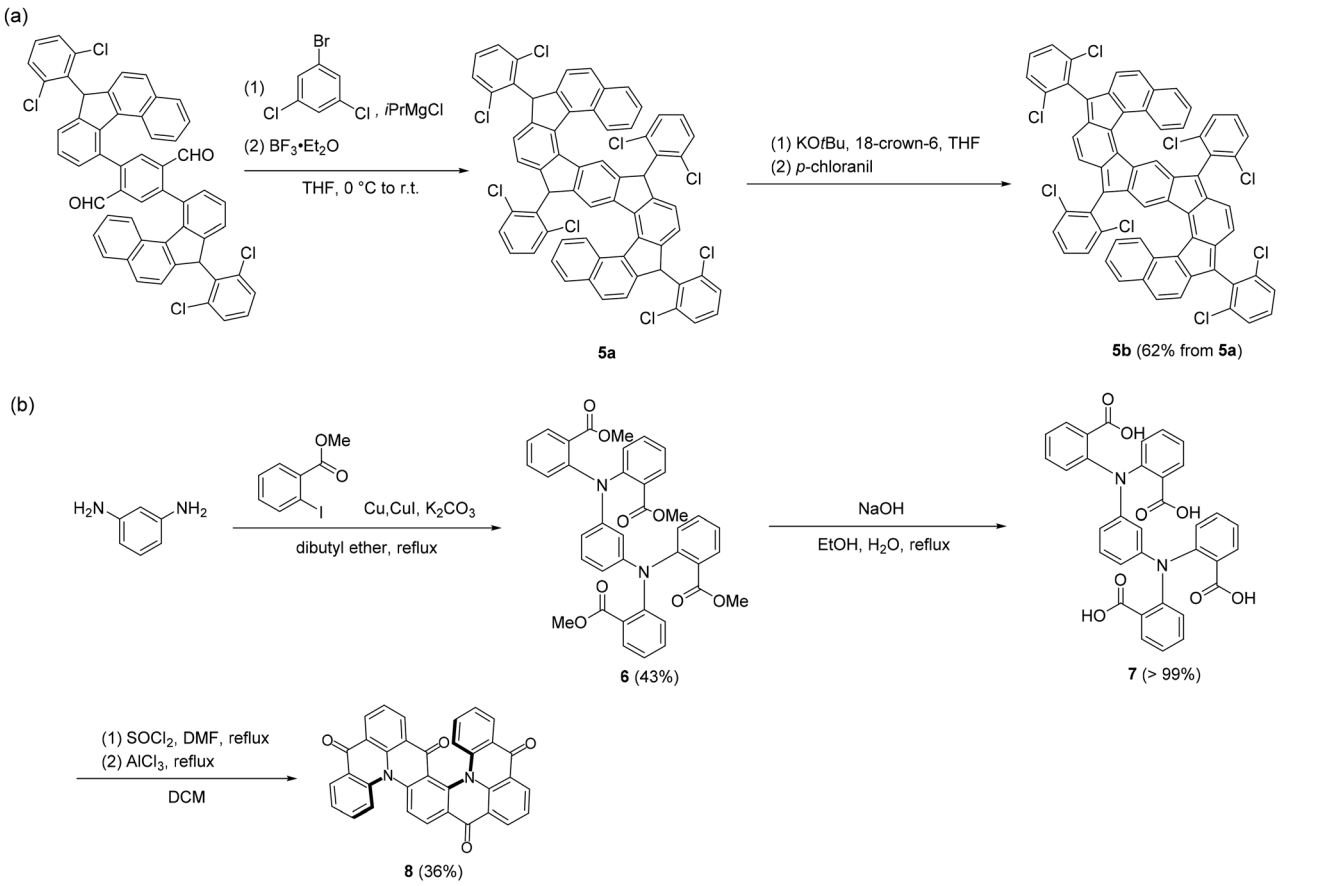

Fig. 3 Synthesis of S-shaped double helicenes *via* a Friedel–Crafts reaction.

Consequently, compound **9** was prepared from 12*H*-benzo[*a*] phenothiazine and 2-chloro-1,3-dibromobenzene *via* Buchwald–Hartwig coupling and electrophilic borylation reactions, in a total yield of 12%. This study highlights the significant potential of helicene-based emitters for CP-OLED applications.

2.2 Other linear multiple helicenes

In addition to double helicenes, other multiple helicenes also include linear structural types. In 2021, Nuckolls' research group reported the utilization of perylene diimide in the synthesis of chiral spiral nanoribbons through coupling and ring formation reactions[2,3] (Fig. 5a). Compound **10** is a linear triple helicene, while compounds **11** and **11-iso** are linear quadruple helicenes. To synthesize helicene **10**, the precursor helicene **12**, which contains two perylene diimide (PDI) units, was initially transformed into the bis(pinacolato)diboron-substituted helicene **13**. Subsequent Suzuki–Miyaura cross-coupling reactions, followed by a regioselective photocyclization sequence, led to the formation of the linear triple helicene **10** in an overall yield of 44% in two steps. For the preparation of **11**, two successive Suzuki–Miyaura couplings between aryl bromide **14** and the bis-Bpin reagent **15** were carried out while retaining the *N*-methyliminodiacetic acid (MIDA) protecting group in the substrate. This was followed by two photocyclization steps to produce the bis-MIDA boronate intermediate.

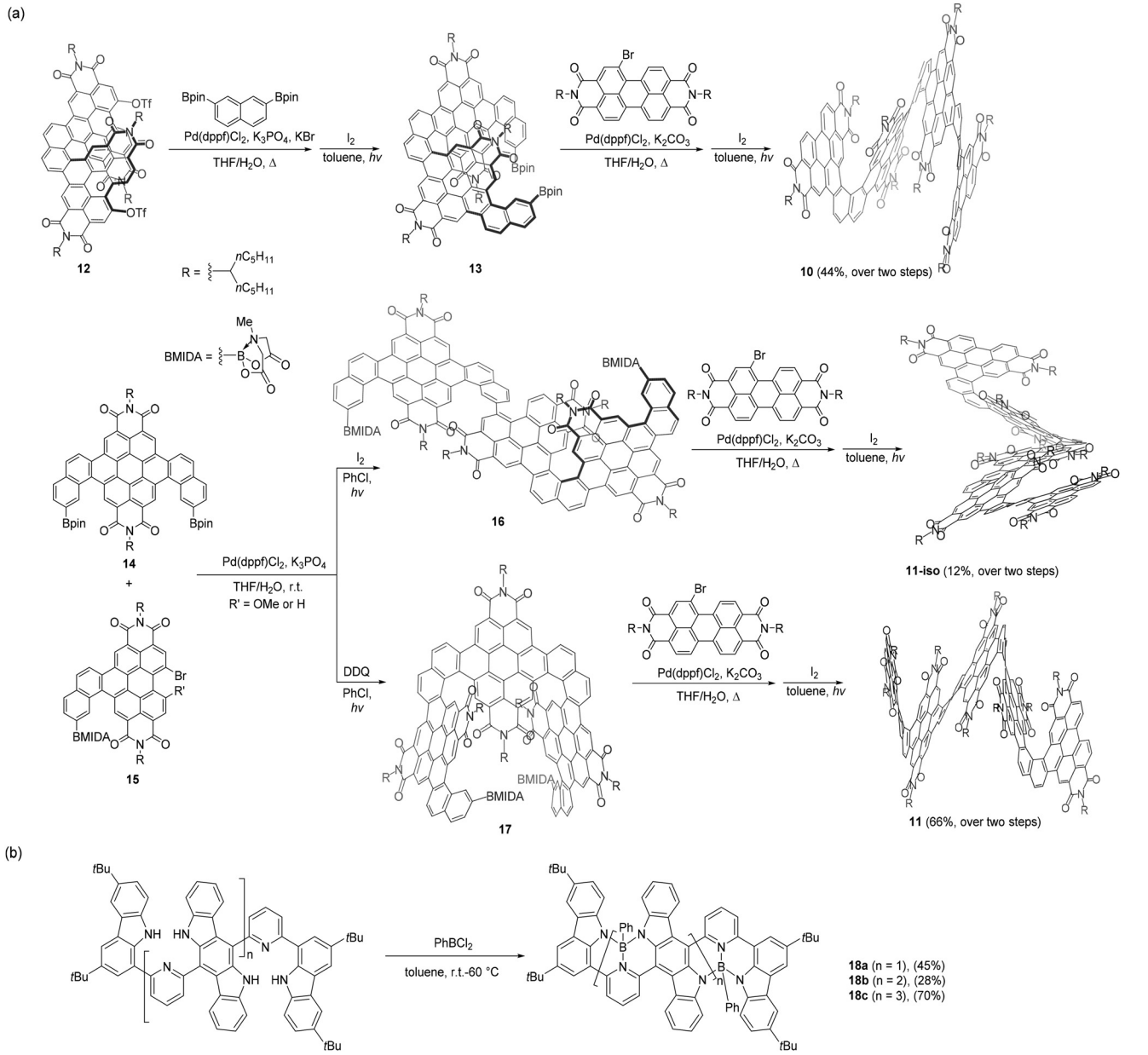

Fig. 5 Synthetic routes to other linear multiple helicenes.

Notably, iodine-mediated photocyclization predominantly yielded compound **16** as the major product, which exhibited resistance to further conversion to **17** even at elevated temperatures. Conversely, photocyclization using 2,3-dichloro-5,6-dicyano-1,4-benzoquinone (DDQ) as an oxidant selectively generated **17** as the primary product. Finally, by employing synthetic procedures similar to those for NP4H, two-step transformations from **16** and **17** resulted in the isolation of the linear quadruple helicenes **11-iso** and **11** in 12% and 66% yields, respectively. This strategy emphasizes the precise regulation of regioselective photocyclization and the sequential construction of complex helical structures using boronate protection techniques. These conjugated chiral molecules exhibit intriguing chemical, biological, and chiral characteristics.

In 2024, Yang's group reported one kind of linear multiple helicene[24] (Fig. 5b). They utilized a new synthetic approach to create a series of boron-bridged helically twisted donor–π-acceptor (D–π-A) conjugated systems. By employing sequential Suzuki coupling reactions, they prepared precursor compounds containing multiple carbazole and pyridine groups. Subsequent electrophilic borylation reactions led to the formation of helical nanobelt compounds **18a–c** in 45%, 28%, and 70% yields, respectively. These boron–nitrogen-doped multiple helicenes exhibited bright red to near-infrared (NIR) emission, opening up avenues for developing advanced materials with tailored optoelectronic properties, especially in the challenging NIR spectral region. This accomplishment underscores the promise of boron-mediated helical structures in diversifying the functionality of π-conjugated systems.

3 Cyclic multiple helicenes

Cyclic multiple helicenes are defined by a cyclic structure made up of multiple helicene units. This structure can be constructed by connecting helicene units end-to-end to form a closed-ring conjugated system or by bridging the termini to create rings, which then twist into multiple helicene configurations. The closed-ring architecture and intrinsic cavity of cyclic multiple helicenes make them promising for applications in molecular recognition and photoelectric fields. As a result, research interest in these compounds has surged in recent years.

In 2017, Osuka's group unexpectedly synthesized a closed hexathia-double [9]/[5]helicene *via* Scholl oxidation of an *o*-phenylene-bridged hexathiophene precursor[25] (Fig. 6a). This process involved a 1,2-aryl migration of a thiophene-linked benzene unit, forming new C–C bonds between α- and β-carbon atoms of adjacent thiophene units. The macrocyclic double helicene **19** was achieved in 66% yield. The oxidative cyclization demonstrated high selectivity, primarily producing the double helicene. This unique asymmetric double-helical structure marks a significant advancement in helicene chemistry by introducing a novel non-planar π-conjugated framework, enhancing structural diversity in the field.

By employing "head-to-head" and "tail-to-tail" connection, two individual helical olefin units are integrated into cyclic molecules, effectively anchoring the end of the helical olefin to minimize racemization and stabilize the helical configuration. In 2017, Durola's group successfully synthesized a double helicene with a macrocyclic structure[26] (Fig. 6b). The macrocyclic compound **20** was thus synthesized *via* a quadruple Perkin condensation reaction involving diphenylglyoxalic acid and terephthalic acid in a diluted solution, resulting in 21% isolated yield. Subsequent quadruple oxidative photocyclization reactions produced the double helicene **21** with a closed macrocyclic architecture in 54% yield. Analysis using X-ray crystallography confirmed its unique non-planar geometry. This study showcased a systematic approach to building intricate helical frameworks through the consecutive condensation and photocyclization processes, broadening the scope for designing novel topologically distinct π-conjugated systems.

In 2024, Zhang's group successfully synthesized a persistent chiral cyclic double helicene using a cove-region bridging strategy[27] (Fig. 6c). The double helicene produced through this approach exhibits a compact 3D cavity. The synthesis of this target compound was achieved by leveraging the structure of a known double heterohelicene. In the spiro-phenazine (SPZ) molecule, the presence of steric hindrance in the cove region causes the two benzene rings connected to the phenazine (PZ) unit to orient either upwards or downwards relative to the PZ unit, resulting in the formation of (*P*,*P*) and (*M*,*M*)-enantiomers. To bridge the cove region of SPZ, dibromo-SPZ (DBrSPZ) was initially synthesized as a crucial intermediate. Subsequently, a lithium-halogen exchange reaction was conducted at −78 °C using *n*-BuLi as the lithiating agent. The macrocyclic structures of **22** and **23** were successfully obtained in 56% and 49% yields, respectively, by reacting the prepared dilithium reagent with terephthaloyl/isophthalyl dichloride. Subsequently, using BH_3 and Et_3SiH as reducing agents in two sequential reduction steps, the double helicene **24** was obtained in a total yield of 17%. The macrocyclic structural features endow these compounds with persistent chirality. Moreover, the cyclic double helicenes possess excellent luminescence properties, including thermally activated delayed fluorescence and circularly polarized luminescence.

4 Cross-linked multiple helicenes

Cross-linked multiple helicenes feature three-dimensional frameworks with the multiple helicene units converging at a central node to form cross or fan-like structures through shared aryl units. This class of compounds include various subclasses, which vary based on the number of spiroene units and the specific aryl units in the common connecting portion.

4.1 X-shaped double helicenes

X-shaped double helicenes consist of two helicene units connected through a distinct cross-linking, forming a spatially crossed configuration resembling the letter "X". This structure often involves shared aromatic rings or bridged connections, resulting in a complex double-helical topology. Recently,

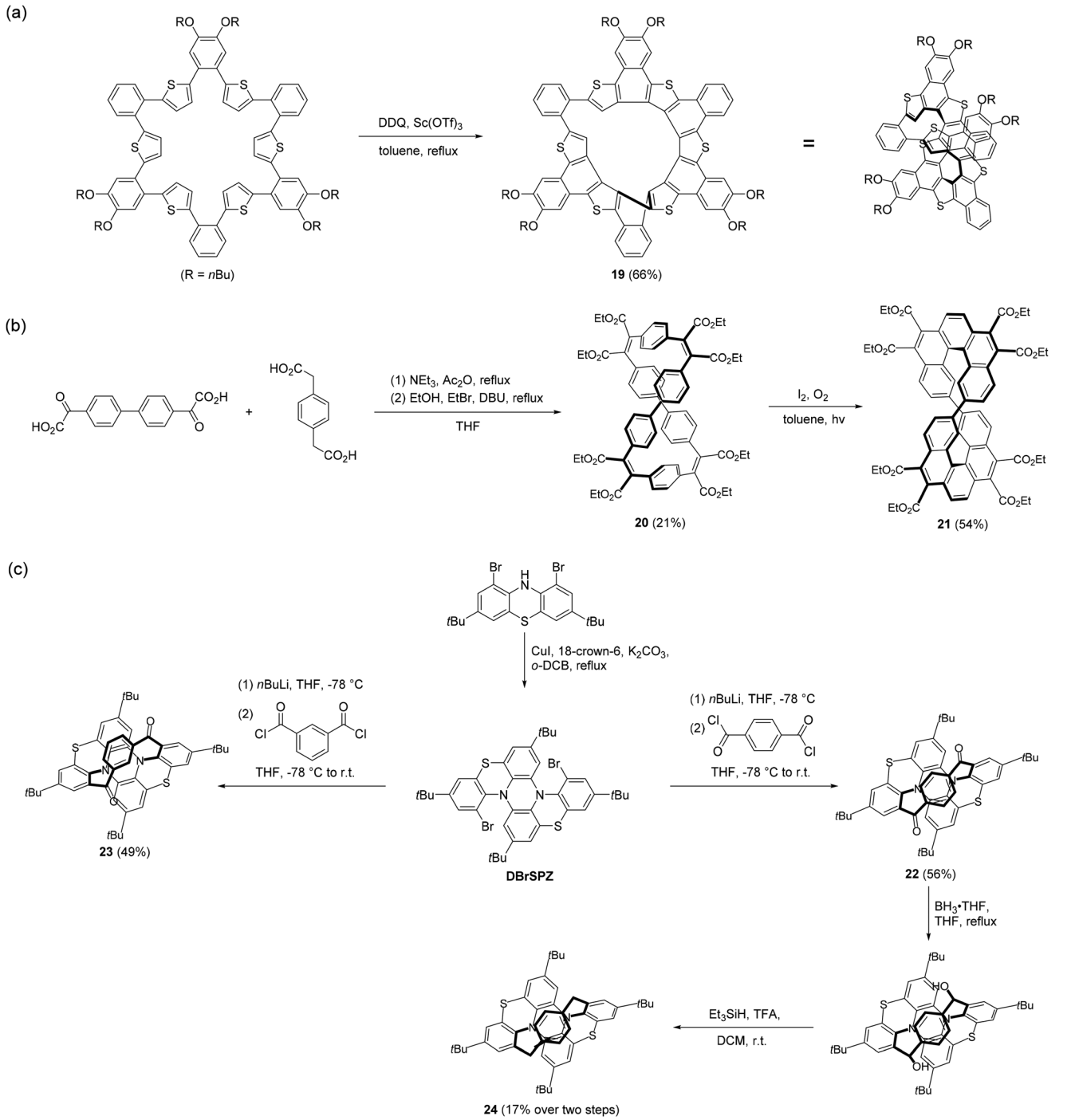

Fig. 6 Synthetic routes to cyclic multiple helicenes.

numerous reports have detailed the synthesis of X-shaped double helicenes.

The synthetic approach of utilizing benzene rings as aromatic cores to create X-shaped cross-conjugated double helicenes by connecting two molecular fragments through a common benzene ring has gained considerable attention and has been extensively documented in recent literature. In 2019, Zhang and colleagues utilized a palladium-catalyzed Suzuki coupling reaction in conjunction with a highly regioselective intramolecular Scholl reaction to produce boron–nitrogen-doped double [5]helicene **25** and boron–nitrogen-doped double [6]helicene **26** in 83% and 49% yields, respectively[28] (Fig. 7a).

In 2020, Yasuda's group successfully doped boron and nitrogen atoms into a helicene framework at the *para*-position, forming B-π-B and N-π-N patterns around the central benzene ring[29] (Fig. 7b). This modification imparted unique physico-

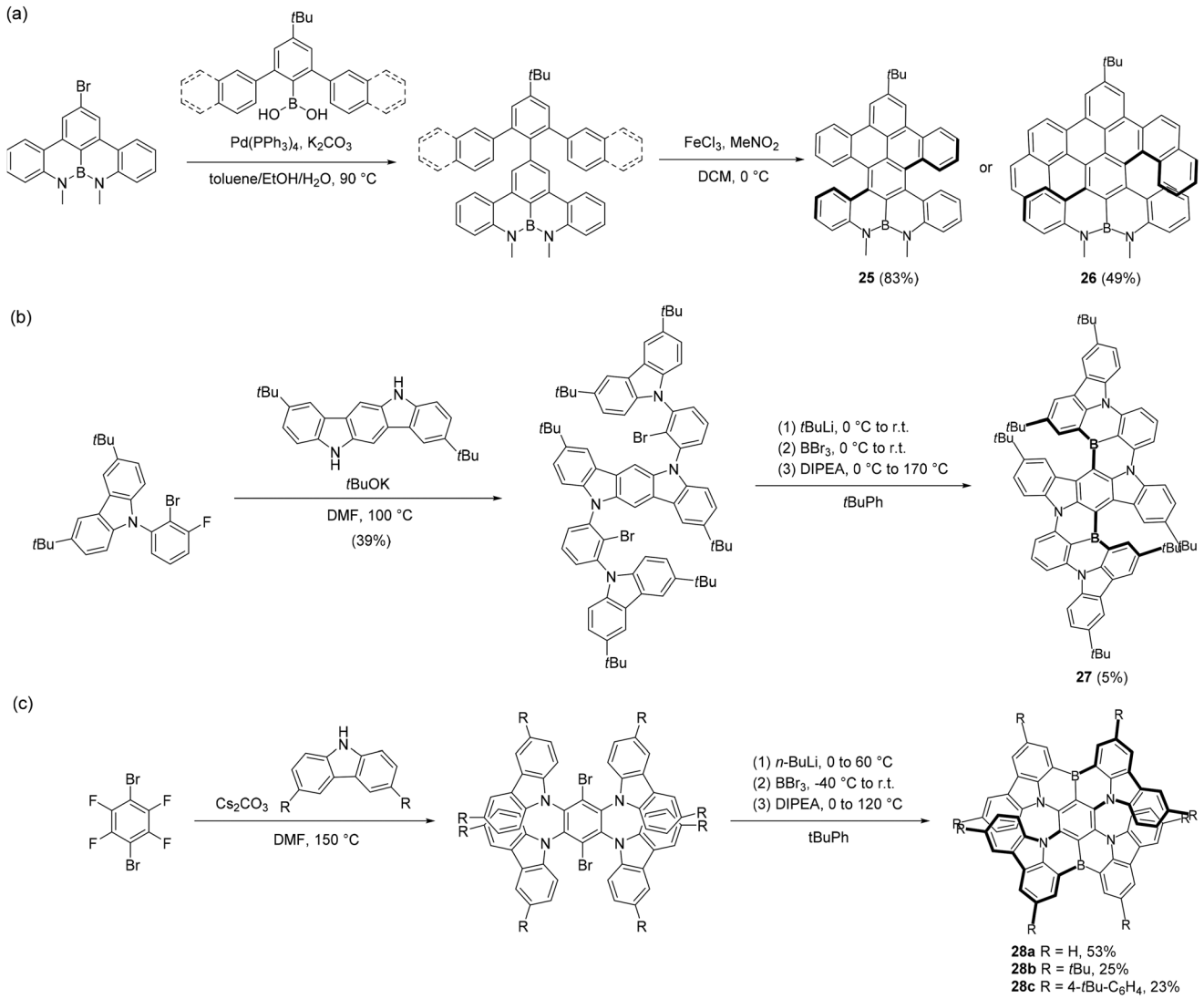

Fig. 7 Synthetic routes to X-shaped B,N-embedded double heterohelicenes.

chemical properties to the boron–nitrogen-doped helicenes. The team initially used carbazole derivatives and indolocarbazole as starting materials, achieving 39% yield of an intermediate *via* nucleophilic substitution. Then, boron nitrogen doped double [6]helicene **27** was obtained by lithium chloride exchange and electrophilic boron acylation, in 5% yield.

In 2021, Wang's group synthesized three B,N-embedded double hetero[7]helicenes with X-type structures[30] (Fig. 7c). The starting material was 1,4-dibromo-2,3,5,6-tetrafluorobenzene, which underwent aromatic nucleophilic substitution reactions with carbazole and its derivatives to yield the corresponding intermediates. Subsequently, by lithium-halogen exchange and electrophilic boration reactions, a "one-pot method" was employed to efficiently incorporate non-bonded boron and nitrogen atoms into the helical skeleton, producing the B,N-embedded double hetero[7]helicenes **28a**, **28b**, and **28c** in 53%, 25%, and 23% yields, respectively. Single-crystal X-ray diffraction analysis revealed that **28b** has a unique double-helix structure with overlapping aromatic rings at the termini. The multiple resonance effects induced by the non-bonded boron and nitrogen atoms in the compounds lead to orbital separation, which is beneficial for improving the absorption asymmetry factor of this type of helicene. This compound demonstrates excellent chiral optical properties, underscoring the significant research value of X-type double helicenes in structural studies.

In 2023, Duan's group synthesized a B,N-doped double helicene with pure red emission featuring an X-shaped crossed topology[31] (Fig. 8a). The synthetic route for B–N bond-embedded hetero-[*n*]helicene **29** involves three reaction steps: starting with nucleophilic substitution, followed by a Suzuki–Miyaura coupling reaction, and culminating in a one-pot borylation/cyclization reaction that delivered the target compound in 45% yield. Substantial steric hindrance between benzene rings induced the formation of a double-helical motif comprising [6]-helicene and [7]-helicene units, with fusion occurring

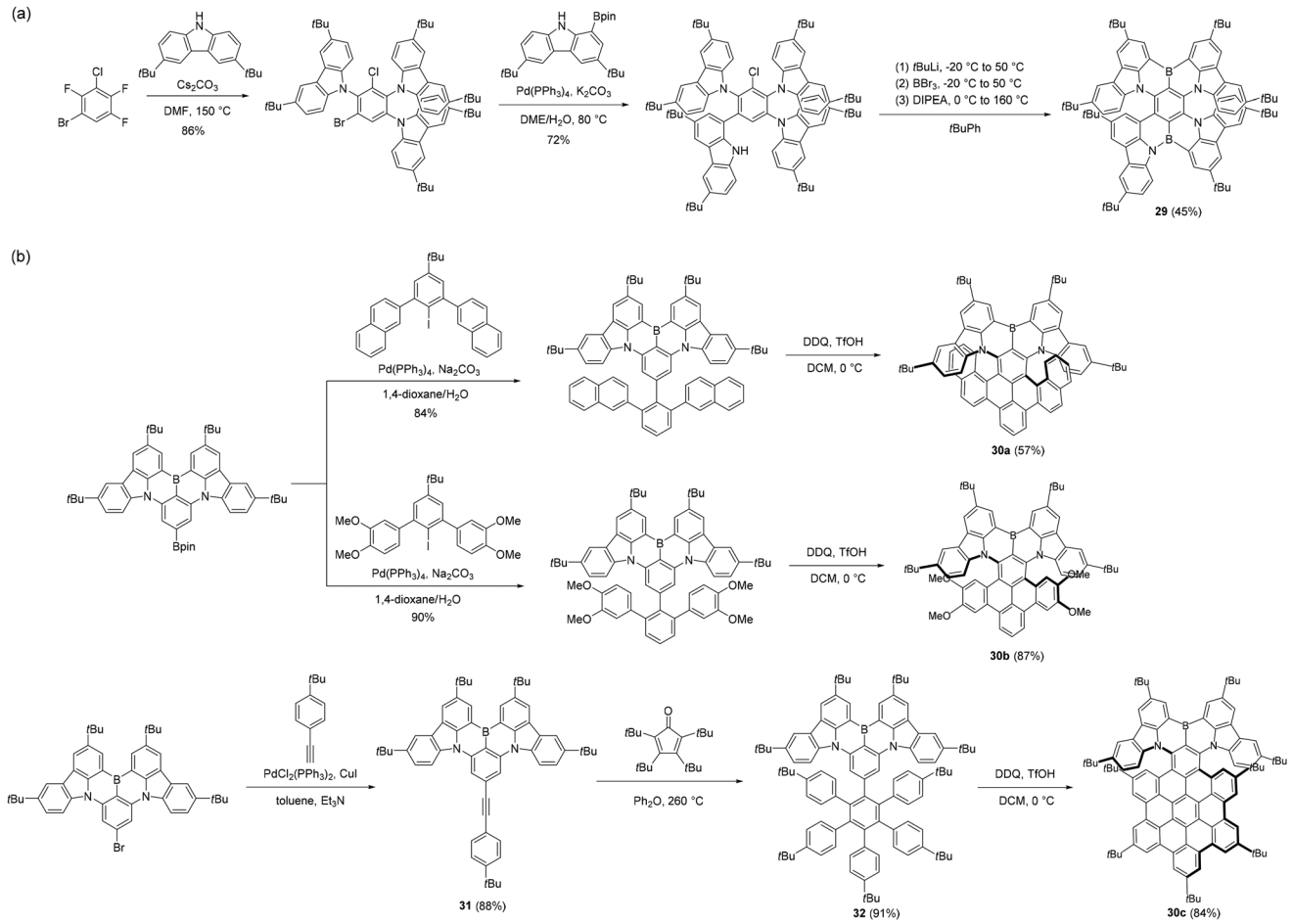

Fig. 8 Synthetic routes to X-shaped B,N-embedded heterohelicenes.

at the benzene hubs to construct the X-shaped crossed architecture. This strategy, achieved through modification of the **28b** scaffold to incorporate a B–N covalent bond, effectively reduced the electron-withdrawing strength of the boron atom and the electron-donating strength of the *para*-positioned nitrogen atom, ultimately yielding the exclusively red-emitting double helicene compound.

In 2024, Tan's group reported their work on the synthesis of B,N-doped nanographenes[32] (Fig. 8b). With D*t*BuCzB-Bpin as the starting material, the double helicenes **30a** and **30b** were synthesized in 57% and 87% yields, respectively, by Suzuki coupling followed by a Scholl reaction. For product **30c**, the precursor **31** was obtained in 88% yield *via* Sonogashira coupling between BN-Br and 4-*tert*-butylphenylacetylene. Subsequently, Diels–Alder cycloaddition between **31** and 2,3,4,5-tetraarylcyclopenta-2,4-dien-1-one afforded precursor **32** in 91% yield. Treatment of **32** with DDQ and TfOH at 0 °C for 0.5 hours gave double [6]helicene **30c** featuring a hexabenzocoronene structure in 84% yield.

The oxidative cyclization of triphenyl-type precursors *via* Scholl reactions has become a powerful method for constructing X-shaped double helicenes. In 2019, Narita and colleagues synthesized π-extended X-shaped double helicenes fused with pyrene units[33] (Fig. 9a). The synthesis began with tetrabromoterphenyl, which underwent Suzuki cross-coupling with 2-pyrenylboronic ester, yielding **33** in 85% yield. A subsequent Scholl reaction mediated by DDQ produced the target double [7]helicene **34** in 10% yield. Single-crystal X-ray analysis revealed significant helical overlap at the molecule's termini, along with pronounced intramolecular and intermolecular π–π interactions due to extended π-conjugation. In 2020, Hu's group synthesized furan-incorporated oxa-double[7]helicenes[34] (Fig. 9b). Using a similar approach, they substituted boronic acid with benzofuran derivatives, achieving intermediate **35** in 87% yield. Subsequent oxidative annulation yielded the X-shaped double [7]helicene **36** in 34% yield. **36** displayed stable twisted conformations at both helical ends.

In 2024, Dou and colleagues synthesized two boron-doped X-shaped double[6]helicenes[35] (Fig. 9c). They employed Suzuki coupling of boron-containing units with a triphenyl-derived diboronate precursor, achieving the helicene precursors **37a** and **37b** in 62% and 10% yields, respectively. Precursor **37a** underwent stepwise Scholl oxidation to produce the X-shaped double [6]helicene **38a** in 6% overall yield, while precursor **37b**

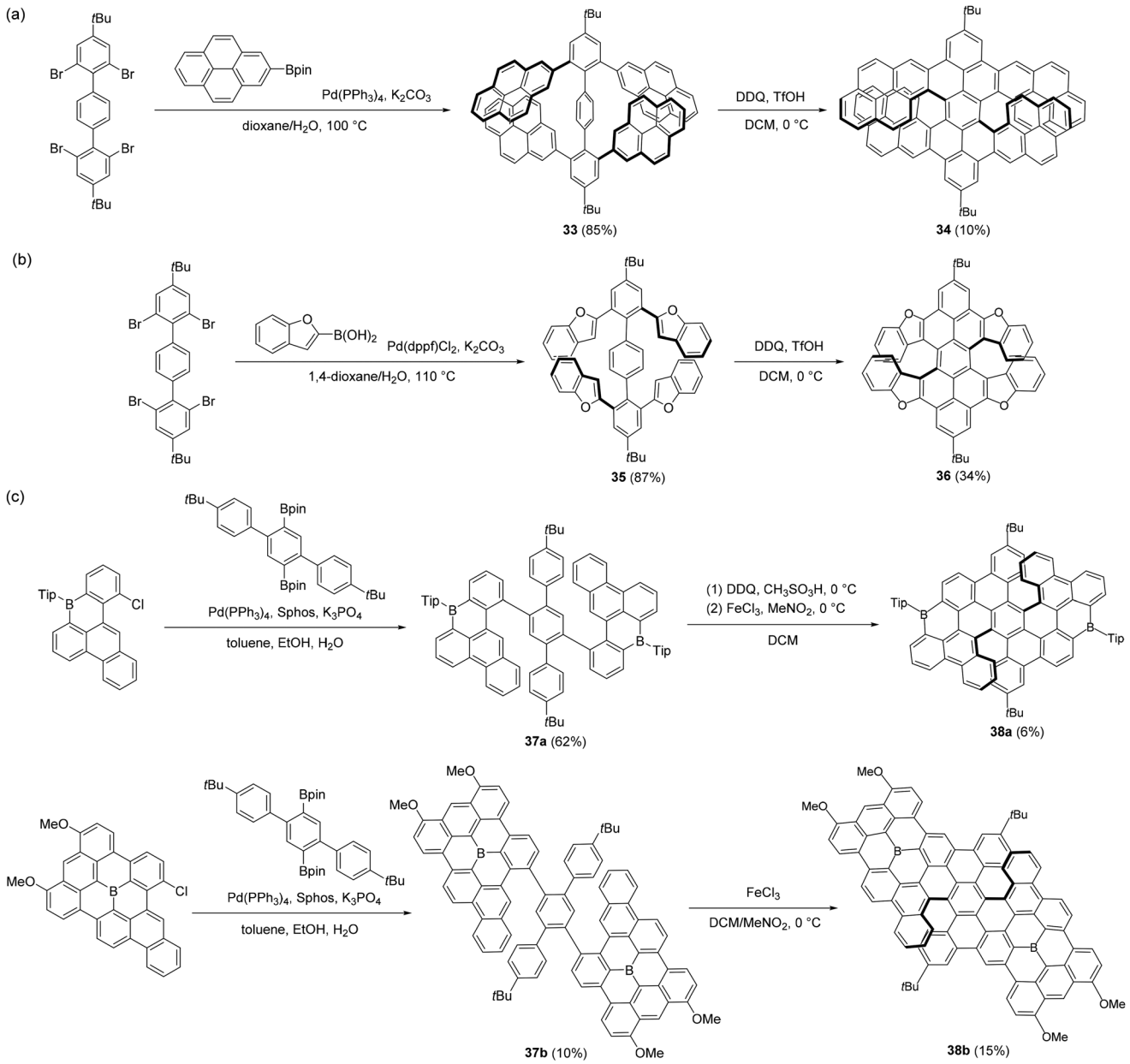

Fig. 9 Synthetic routes to X-type double helicenes using triphenyl compounds as precursors.

was subjected to one-pot Scholl cyclization, yielding the target compound **38b** in 15% yield. Detailed analyses revealed that boron induces delocalized electronic structures within the polycyclic π-system, allowing for tunable photophysical properties in both ground and excited states.

Perylene diimides (PDIs) have attracted considerable interest in organic optoelectronics due to their exceptional properties, including high charge carrier mobility, strong electron affinity, air stability, and versatile molecular design. Incorporating PDI as the aryl core in helicenes to create cross-conjugated helicene compounds is therefore of substantial research interest. In 2018, Wang's group synthesized double helicenes with thiophene heterocycles and a PDI core[36] (Fig. 10a). From the *ortho*-functionalizing PDI, they achieved tetrabromo-substituted intermediates **39a** and **39b** in 62% and 45% yields, respectively. Subsequent alkyne coupling and four-fold thiophene annulation produced the X-shaped double [5]helicenes **41a** and **41b**, which were then converted to products **42a** and **42b** *via* a desilylation reaction using Nu_4NF. In 2021, Lin's group introduced a skeleton-fusion strategy, constructing *ortho*-π-extended PDI-based double-[7]heteroheli-cenes by integrating a twisted PDI core with four fused heteroaromatic rings[37] (Fig. 10b). Using tetraiodo-substituted PDI as the substrate, intermediate **43** was obtained *via* aromatic nucleophilic substitution in 81% yield. Subsequently, a palladium-catalyzed intramolecular C–H activation reaction furnished the tetraindole-fused PDI double helicene in 51% yield.

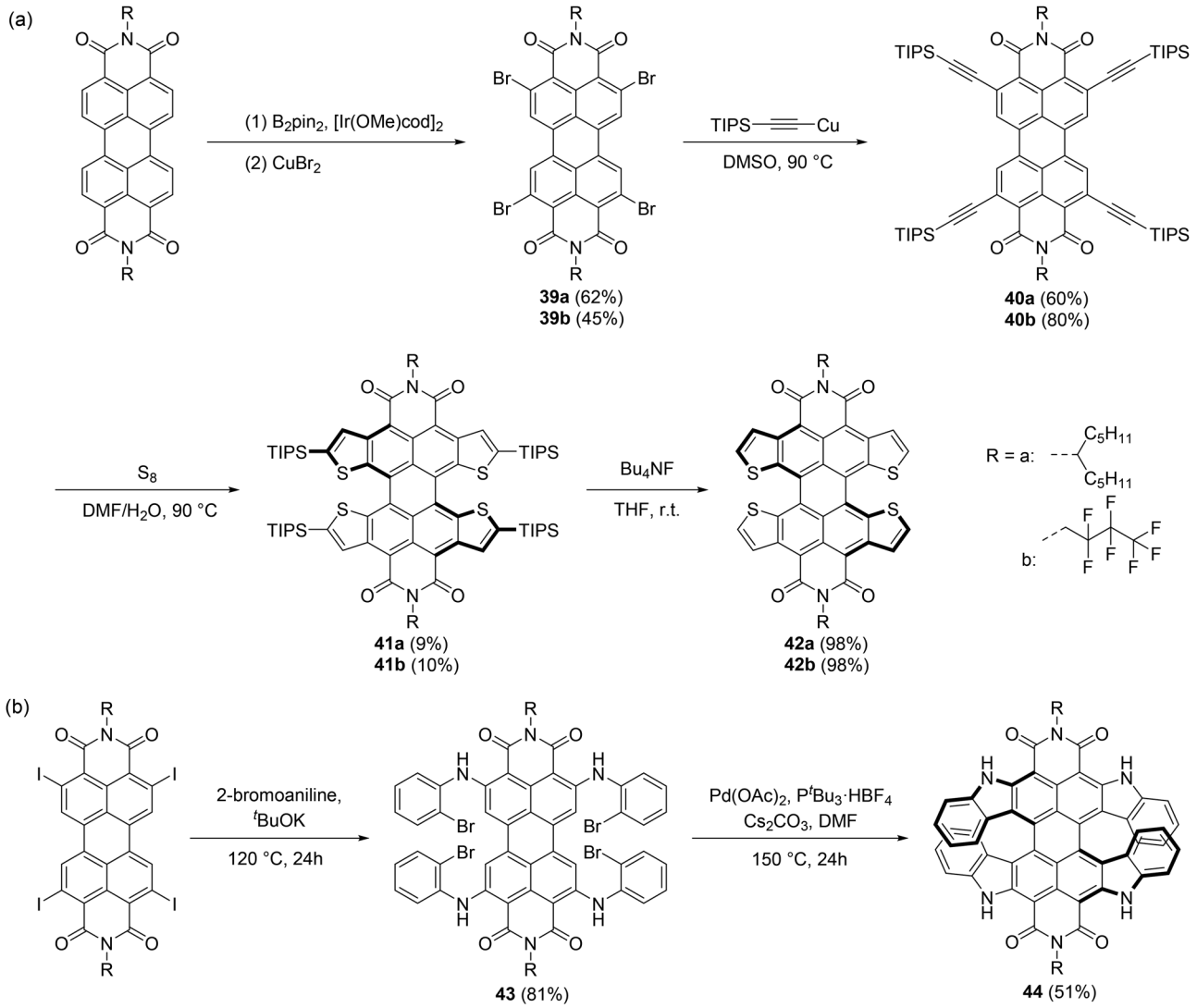

Fig. 10 Synthetic routes to X-type double helicenes with PDI as the core.

Utilizing perylene as the core is an effective strategy for synthesizing twisted nanographenes. In 2022, Qiu's group reported two π-extended chiral nanographenes featuring 29 benzene rings and two helical gaps[38] (Fig. 11a). Consequently, a highly congested perylene-core twisted graphene precursor was synthesized *via* Suzuki coupling between a perylene compound with four boronate ester groups and aryl iodides. Subsequent oxidative cyclization under Scholl reaction conditions showed that the highly strained precursor favored rearrangement to alleviate internal strain, resulting in two cross-shaped double helicene structural isomers **44a** and **44b** in a 5 : 2 ratio in a total yield of 53%. In 2023, Wang's group synthesized a double [6]helicene-type chiral nanographene using a similar synthetic strategy[39] (Fig. 11b). A Suzuki cross-coupling reaction yielded compound **45** in 88% yield. Subsequent cyclization at the *peri* position of perylene under standard Scholl reaction conditions (DDQ/TfOH) produced double [6]helicene **46** in 67% yield. Both the racemate and mesomer were detected, with a ^{1}H NMR-determined **46-*rac*** to **46-*meso*** ratio of 3 : 2. Notably, no cyclization at the bay positions of perylene or rearrangement products were observed, demonstrating the high regioselectivity of the Scholl reaction in this study.

4.2 Cross-linked triple helicenes

Helicene compounds featuring propeller-shaped triple helical structures were synthesized *via ortho*-annulation of three radially extending conjugated segments from a central benzene core. Steric interactions between adjacent units stabilize the triple helical topology.

In 2017, Watanabe *et al.* reported a method for synthesizing triple helicenes using triphosphonates and 2-naphthalaldehyde derivatives as precursors[40] (Fig. 12a). Through Arbuzov reactions, they synthesized the trialkenyl-substituted triple helicene precursors **47a** and **47b** in 48% and 87% yields, respectively. Photocyclization of the methoxy-containing pre-

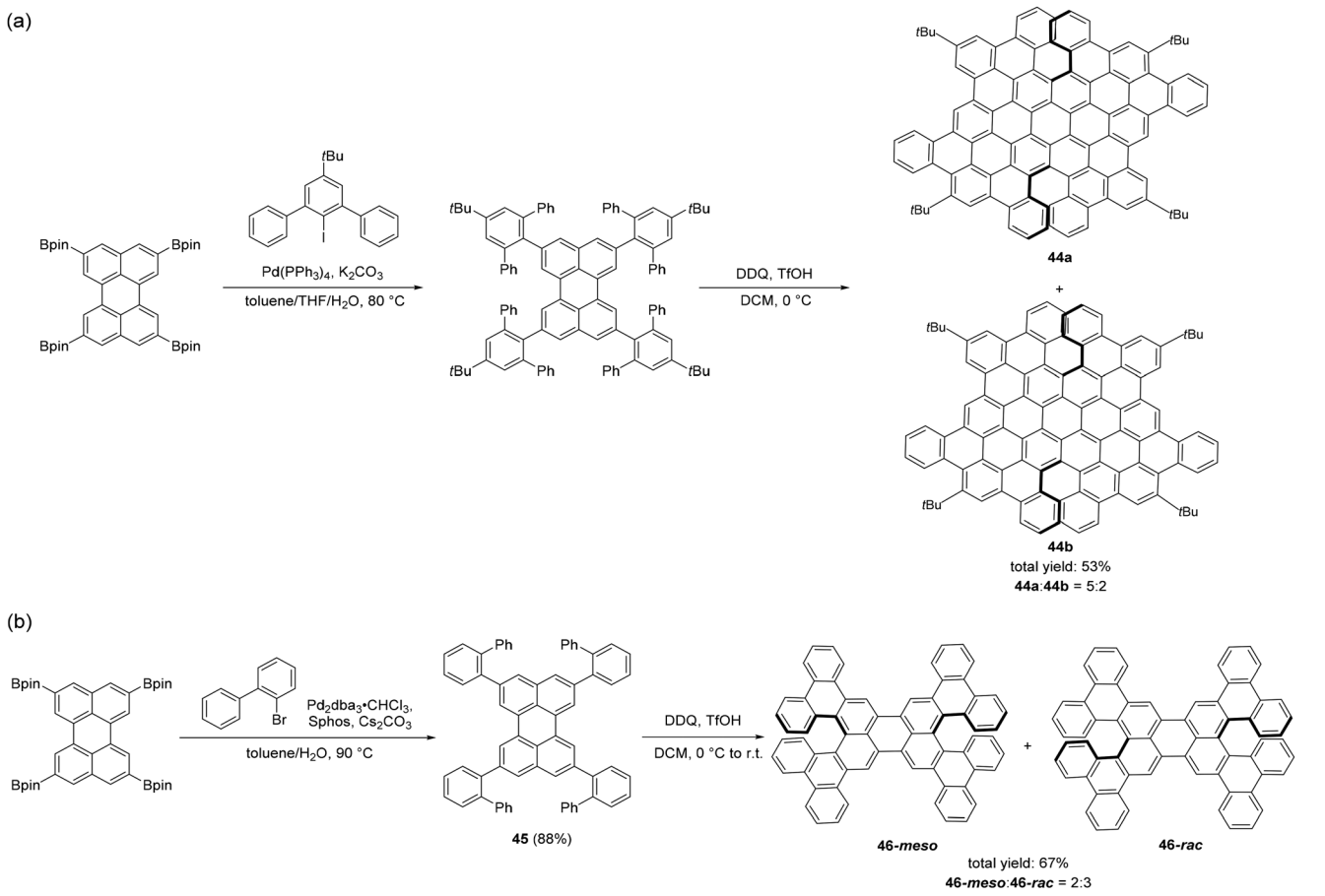

Fig. 11 Synthetic routes to X-type double helicenes with perylene as the core.

cursor **47a** *via* an eliminative pathway under a 450 W high-pressure mercury lamp produced the triple [5]helicene **48** in 37% yield. In contrast, the non-methoxy analogue underwent oxidative photocyclization, yielding the same product in 63% yield.

In 2018, Itami's group[41] synthesized a C3-symmetric, propeller-shaped triple [4]helicene with three heptagonal rings through a two-step process (Fig. 12b). The initial Suzuki coupling yielded precursor **49** in 68% yield, followed by a palladium-catalyzed intramolecular C–H arylation to achieve construction of the triple [4]helicene **50**. The reaction favored the formation of a heptacyclic system over the expected hexacyclic triple [6]helicene, likely due to steric repulsion among [6]helicene subunits in the intermediate. Computational analysis indicated that the incorporation of heptagonal rings significantly stabilized the helicity of the [4]helicene system.

In 2022, Zhang's team introduced two novel π-extended triple [5]helicenes[42] (Fig. 12c). Their synthetic process involves precursor assembly, followed by nickel-mediated [2 + 2 + 2] cyclotrimerization, affording intermediates **51a** and **51b** in 70% and 60% yields, respectively. Then, a Scholl oxidative coupling reaction was carried out with $FeCl_3$ to generate the triple helicenes **52a** and **52b** in 60% and 70% yields, respectively. Spectroscopic analysis, single-crystal X-ray diffraction, and DFT calculations verified the C1-symmetric conformation in the crystalline state. In 2023, Liu *et al.* synthesized the triple helicene **53** using a one-pot sequence of Suzuki coupling and Knoevenagel condensation, achieving 26% yield[43] (Fig. 12d). Subsequent nitration with $NOBF_4$ produced the C3-symmetric **54** in 40% yield. Notably, **54** formed hierarchical (PPP·PPM·MMP·MMM) tetrameric stacks in the solid state, exemplifying a rare social self-sorting behavior. This study establishes fundamental structure–property relationships in fused polycyclic helicene systems.

Synthesizing heterocyclic-containing triple helicenes remains a significant challenge. In 2021, You's group reported the synthesis of a furan-based triple oxa[7]helicene[44] (Fig. 13a). The process began with brominated benzofuran preparation, followed by alkynylation with propiolic acid to yield a diarylacetylene substrate. A subsequent [2 + 2 + 2] cyclotrimerization, catalyzed by octacarbonyldicobalt, produced the hexaarylbenzene precursor **55** in 56% yield. Finally, intramolecular cyclization using $FeCl_3$ and DDQ at 60 °C afforded the triple oxa[7]helicene **56** in 49% yield. Compared to previously reported double oxa[7]helicenes, the triple oxa[7]helicene showed both theoretical and experimental improvements in the lumine-

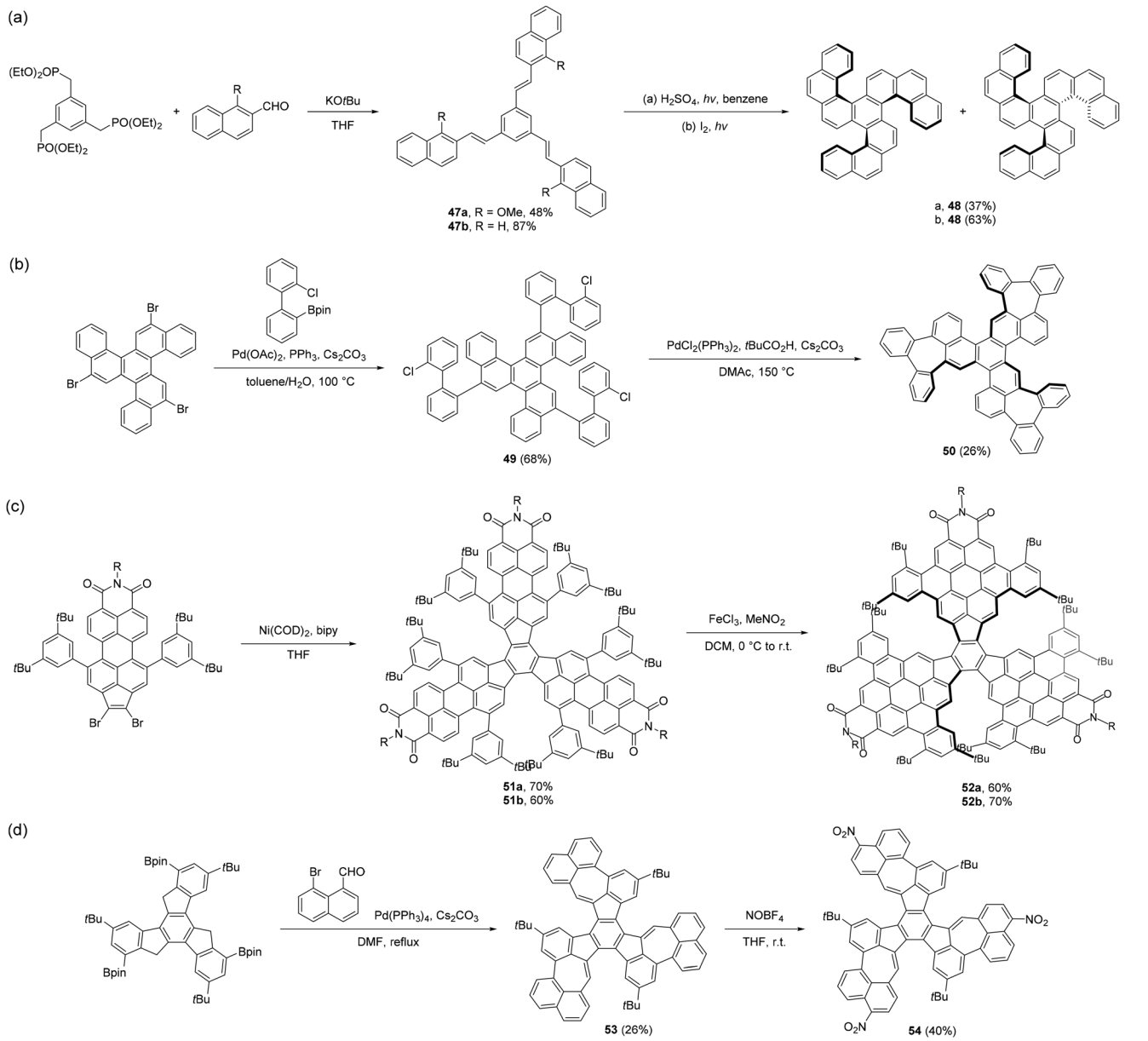

Fig. 12 Synthetic routes to cross-linked triple helicenes.

scence dissymmetry factor, indicating that increasing helicene subunits could enhance the luminescence dissymmetry factor of heterohelicenes.

In 2022, Hu's group synthesized and characterized the first C3-symmetric triple oxa[6]helicene[45] (Fig. 13b). The synthesis of **57** involved two steps. Initially, a triple Suzuki–Miyaura coupling produced intermediate **58** in 75% yield. Then, in the presence of DDQ, the Scholl reaction was carried out in dichloromethane and trifluoromethanesulfonic acid (TfOH) to obtain the triple helicene **57** in 34% yield. Compared to the D3-symmetric triple oxa[7]helicene **56**, the C3-symmetric variant showed parallel electric and magnetic transition dipole moments, enhancing luminescence dissymmetry and highlighting the importance of molecular symmetry in chiral responses. Additionally, the synthesis of sulfur- and selenium-containing propeller-shaped triple helicenes has also been documented. In 2022, Wang's group[46] reported an efficient synthesis of four thiophene/selenophene-based triple[6]helicenes (Fig. 13c). The crucial step was the oxidative photocyclization of intermediates **61a–d** in anhydrous toluene with iodine, producing the target propeller-shaped triple[6]helicenes **62a–d** in 8–35% yields. Replacing sulfur with selenium in the molecular framework altered the racemic triple[6]helicenes' crystal packing due to the changes in intermolecular interactions. Spectroscopic and physicochemical analyses revealed that selenium substitution precisely modulates their luminescence property and molecular energy levels.

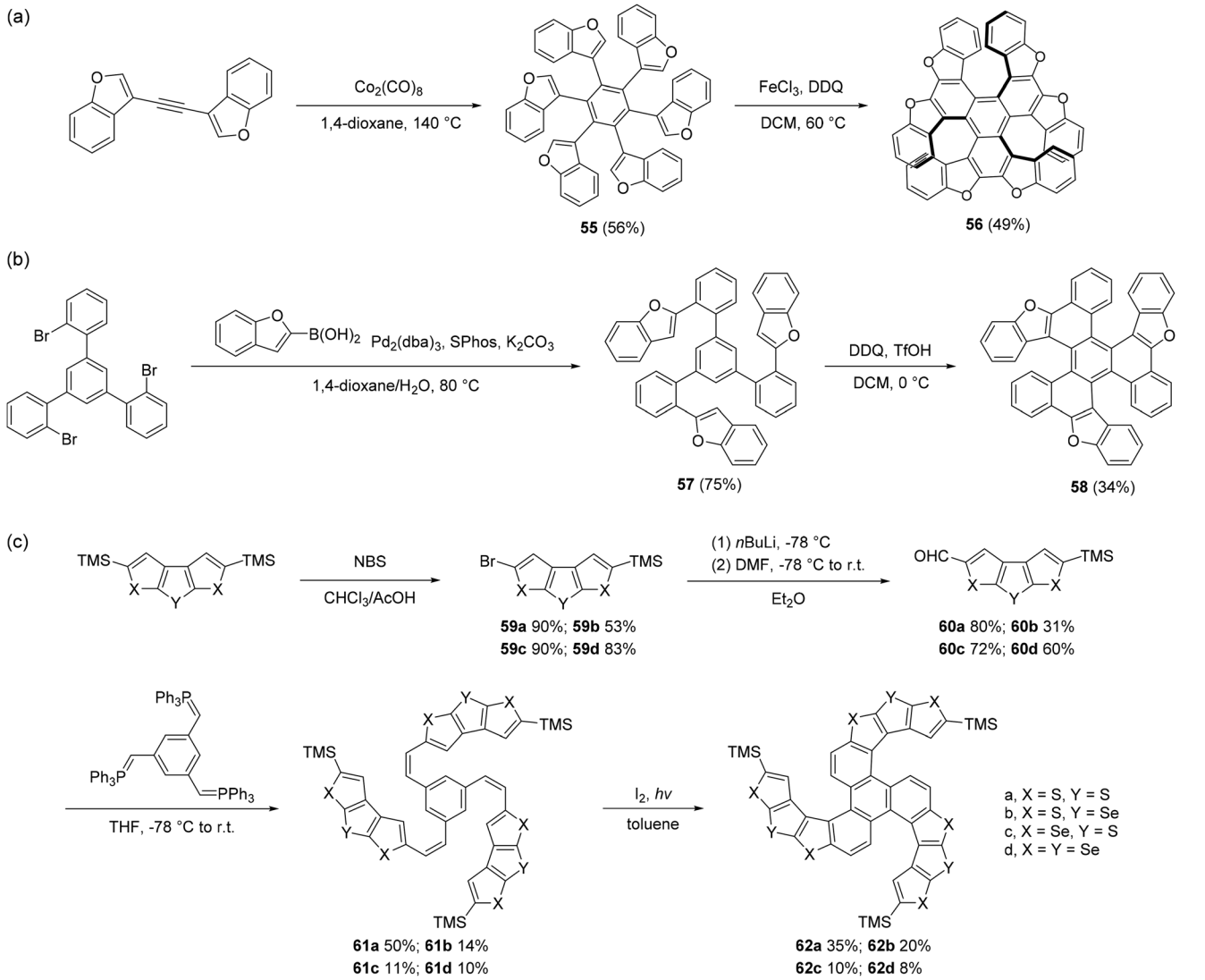

Fig. 13 Synthetic routes to heterocyclic-containing cross-linked triple helicenes.

4.3 Cross-linked quintuple helicenes

Corannulene, as the smallest fragment of C_{60}, exhibits unique properties due to its bowl-shaped geometry and distinctive dynamic behavior, making it highly significant for constructing crossed, fan-shaped multiple helicenes. In 2018, Itami's group reported the synthesis of the first quintuple helicene centered on corannulene[47] (Fig. 14a). Starting from pentaboronate-substituted corannulene, the target compound **63** was obtained in 76% yield *via* five Suzuki–Miyaura coupling reactions with 2-bromo-2′-chlorobiphenyl. Subsequently, in the presence of $PdCl_2(PCy_3)_2$ and DBU, **63** in DMAc solution was stirred at 140 °C for 3 days, resulting in the quintuple [6]helicene **64** in 10% yield.

Similarly, in 2019, using perylene diimide as a component, Wang and colleagues[48] synthesized a new cross-linked quintuple [6]helicene **66** featuring a nonplanar graphenoid structure (Fig. 14b). The synthesis of compound **66** involved two key steps: first, a Suzuki–Miyaura coupling afforded the corannulene-core precursor **65** in 60% yield; subsequently, a photocyclization reaction afforded the target product **66** in 62% yield. Theoretically, **66** possesses eight possible stereoisomers. However, ^{1}H NMR analysis indicated that the photocyclization reaction produced two major diastereomers: (*P*,*P*,*P*,*P*,*P*)-**66** with D_6 symmetry and (*P*,*P*,*P*,*P*,*M*)-**66** with C_2 symmetry.

In 2024, Zhang and colleagues[49] adopted an alternative substrate strategy to synthesize two corannulene-centered quintuple helicenes (Fig. 14c). Using pentaiodocorannulene as the starting material, two types of aryl olefins underwent five Heck reactions, yielding two quintuple helicene precursors **67a** and **67b** in 26% and 38% yields, respectively. Under Mallory reaction conditions, these precursors were converted to the corresponding quintuple [6]helicenes **68a-1** and **68a-2** and the [7]helicene **68b**. Notably, **68b** is the highest reported helicene based on corannulene. X-ray crystallographic analysis revealed

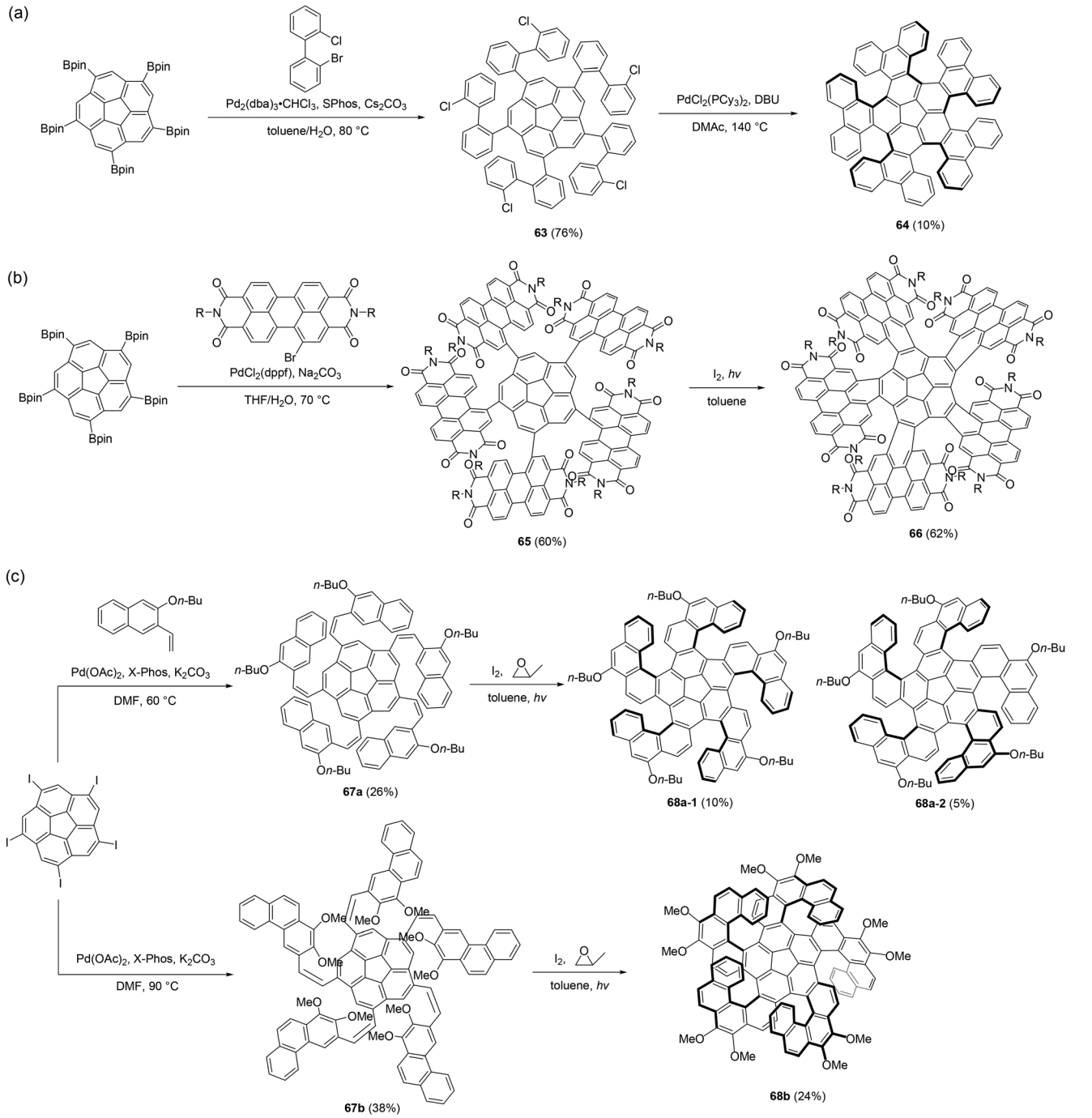

Fig. 14 Synthetic routes to cross-linked quintuple helicenes with corannulene as the core.

that **68a-1** adopts a propeller-like conformation with an intact corannulene core, whereas **68a-2** and **68b** exhibit quasi-propeller conformations.

Similar to corannulene, azabuckybowl also possesses a rigid bowl-shaped structure. Due to the unique photophysical properties arising from nitrogen atom doping in multiple helicene frameworks, the synthesis of cross-conjugated multiple helicenes with an azabuckybowl as the core has been reported in recent years. In 2022, Zheng and coworkers[50] reported the first synthesis of a quintuple helicene centered on an azabuckybowl (Fig. 15a). Thus, **71** was synthesized from an azabuckybowl *via* a three-step reaction sequence. Initially, an iridium-catalyzed borylation reaction between the azabuckybowl compound and $Bpin_2$ afforded the pentaborylated precursor **69** in 75% yield. Subsequently, five consecutive Suzuki–Miyaura coupling reactions yielded precursor **70** in 52% yield. Finally, a

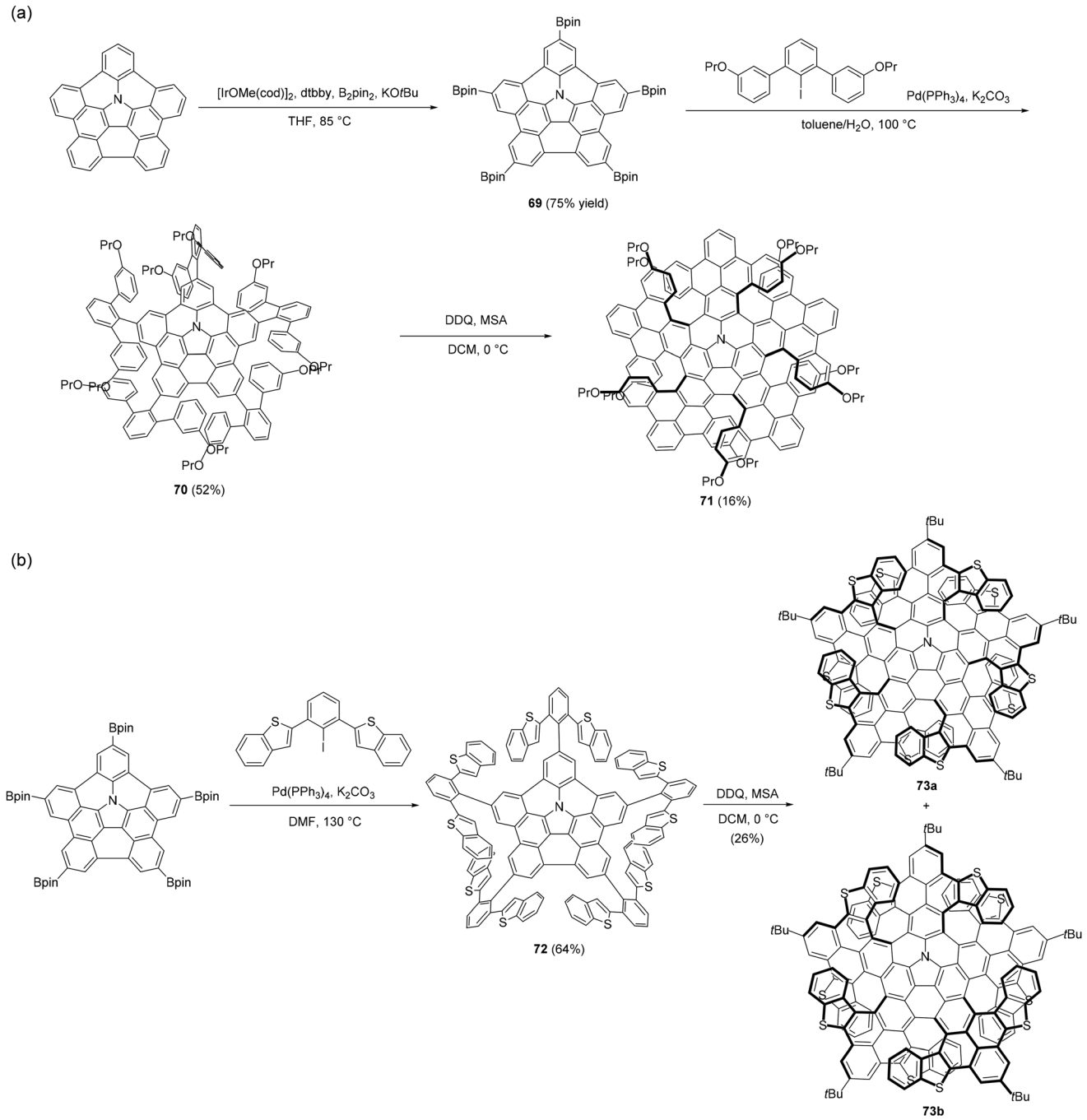

Fig. 15 Synthetic routes to cross-linked quintuple helicenes with azabuckybowl as the core.

Scholl reaction mediated by DDQ and methanesulfonic acid (MSA) produced the target quintuple [7]helicene **71** in 16% yield. It was found that **71** exhibits excellent photophysical properties and inherent chirality, indicating that nitrogen-embedded azacorannulene can serve as an outstanding nitrogen-doped core for constructing novel multiple helicenes with broad application potential. By using a similar synthetic strategy, in 2022, they[51] obtained two conformational isomers of a quintuple [9]helicene centered on an azabuckybowl by introducing thiophene, representing the highest hetero-helicene reported in the field of multiple [*n*]helicenes (Fig. 15b). X-ray crystal structure showed that the quintuple [9]helicene includes not only the propeller-shaped conformational isomer **73a** but also an unforeseen quasi-propeller-shaped conformational isomer **73b**. This is the first time that different conformational isomers have been observed in high-order multiple helicenes ($n > 8$), which might be caused by the doping of heteroatomic sulfur in the helical skeleton.

4.4 Cross-linked hexapole helicenes

Hexabenzocoronene (HBC) is the smallest planar nanographene fragment, and its incorporation as a central motif in the synthesis of cross-shaped multiple helicene-type twisted nanographenes has been increasingly reported in recent years. The synthesis of such compounds primarily involves Co-catalyzed bis(aryl)acetylene [2 + 2 + 2] cycloaddition to construct precursors, followed by oxidative cyclization. In 2018, Wang *et al.*[52] reported the synthesis of cross-linked hexaole [7]helicenes with an HBC core (Fig. 16a). The synthetic route for obtaining **75a** and **75b** comprises two key steps: first, a $Co_2(CO)_8$-catalyzed [2 + 2 + 2] cycloaddition to build two precursors consisting of 25 benzene rings organized on a hexaphenylbenzene (HPB) scaffold; second, a Scholl reaction of the precursor in

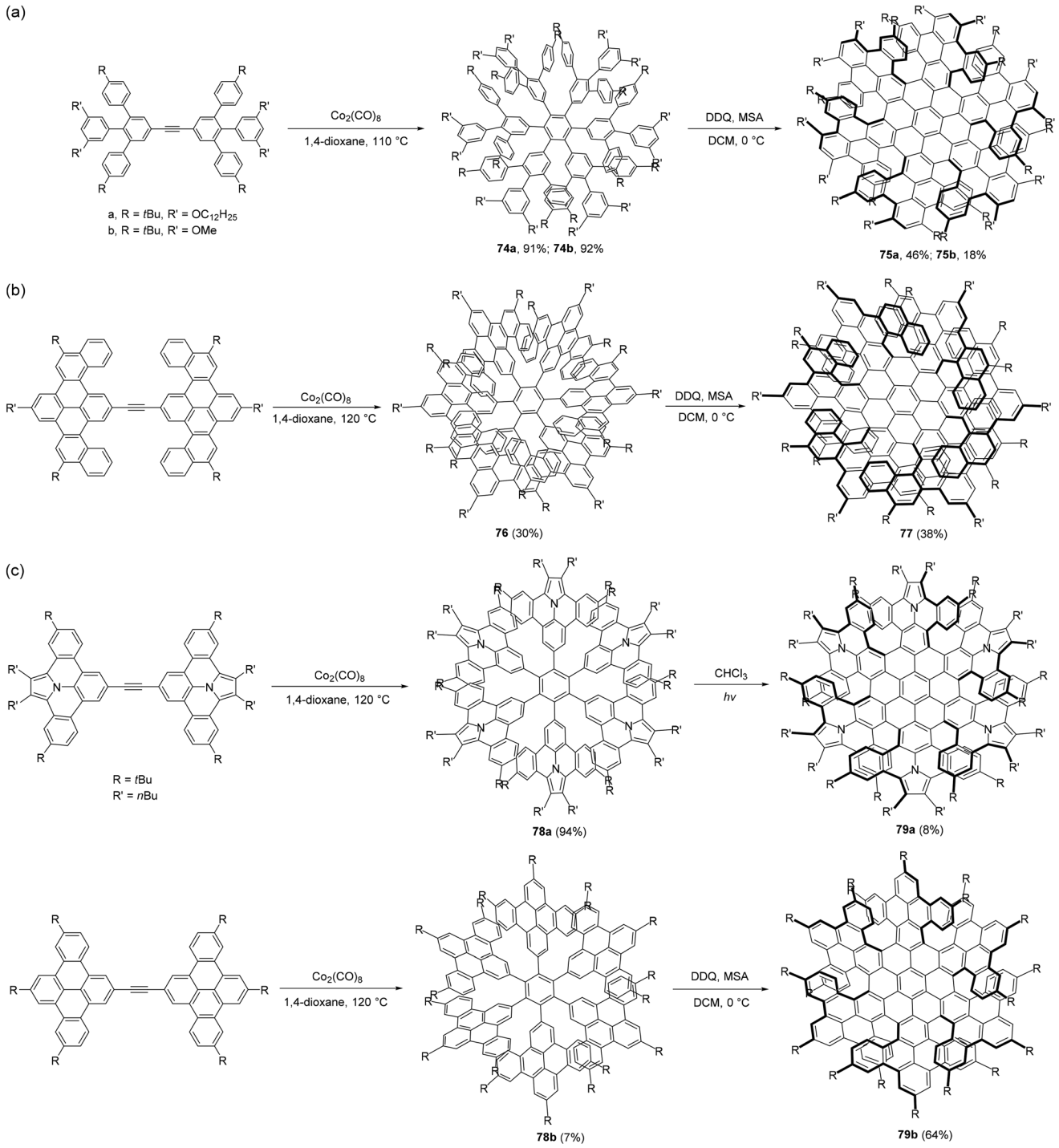

Fig. 16 Synthetic routes to cross-linked hexapole helicenes with hexabenzocoronene as the core.

the presence of MSA and DDQ, yielding **75a** in 46% yield and **75b** in 16% yield. X-ray crystallography revealed that **75a** adopts a propeller-shaped geometry, with six blades fused to the HBC core, each uniformly tilted.

Following a similar synthetic strategy, Wang's group reported a series of hexapole helicene compounds with propeller-shaped structures.[53] As shown in Fig. 16b, by using dinaphthopyrene (DPN) as the terminal arylacetylene units, a Co-catalyzed [2 + 2 + 2] trimerization afforded precursor **76** bearing six DPN fragments. Subsequent oxidative cyclization *via* a Scholl reaction yielded the hexapole [9]helicene **77** in 38% yield, representing the highest-order all-carbon multiple helicene reported to date. Single-crystal analysis showed that the six DPN blades are uniformly tilted, with an average dihedral angle (DA) of ~32°. Due to severe steric repulsion between the crowded blades, the six aryl fragments at the periphery of the HBC core exhibit significant distortion, with an average non-planarity value of 0.128 Å. Furthermore, nitrogen-doped hexapole [7]helicenes were successfully synthesized by employing nitrogen-containing aryl fragments as terminal arylacetylene units[54] (Fig. 16c). When precursors containing nitrogen moieties and their all-carbon analogs were subjected to Co-catalyzed trimerization, two helicene precursors **78a** and **78b** were obtained in 94% and 7% yields, respectively. However, the subsequent oxidative cyclization conditions differed. For precursor **78a**, photocyclization in $CHCl_3$ solution afforded the target compound **79a** in only 8% yield, whereas the other precursor **78b** underwent a traditional Scholl reaction, yielding the target molecule **79b** in 64% yield. Both products exhibited a propeller-shaped geometry with similar crystallographic parameters.

To further expand the π-conjugated system of such hexapole helicenes, Wang *et al.* reported the synthesis of π-extended hexapole [7]helicenes in 2019[55] (Fig. 17). The synthetic route involved two key steps: first, sixfold Diels–Alder addition between compound **80** and cyclohexenone to afford **81** containing six HPB units; second, a stepwise Scholl reaction by treatment with DDQ and TfOH at 0 °C for 1.5 hours to form an

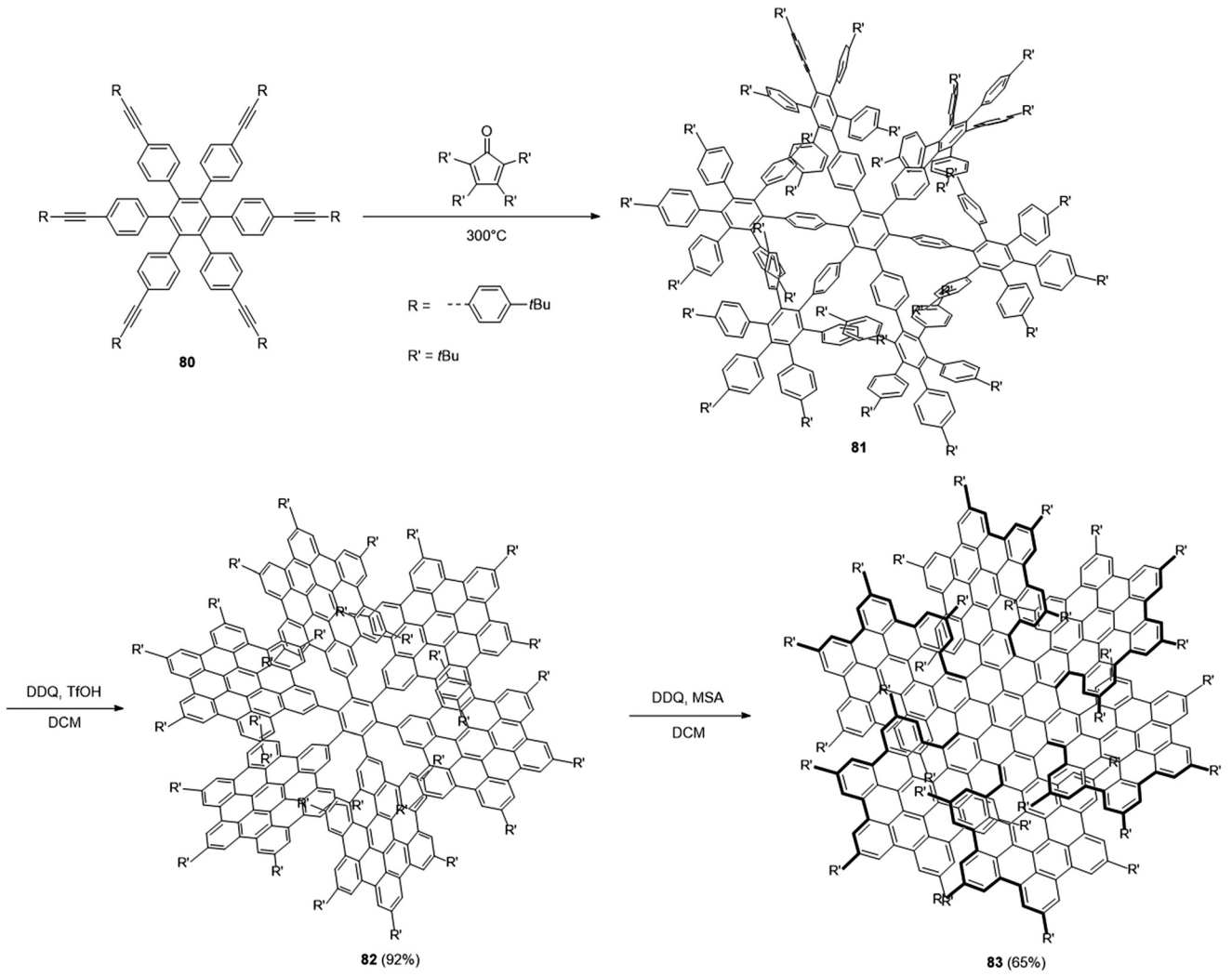

Fig. 17 Synthetic routes to π-expanded cross-linked hexapole helicenes.

intermediate **82** in 92% yield, followed by a second Scholl reaction in the presence of DDQ and MSA to form the central HBC core, yielding the hexapole [7]helicene **83** in 65% yield. The regioselectivity of the Scholl reactions was attributed to the *tert*-butyl substituents on the peripheral HBC fragments, which lowered the oxidation potential and facilitated the cyclization.

5 Conclusions and outlook

In summary, multiple helicenes represent a fascinating class of chiral polycyclic compounds with diverse and complex stereo-structures, emerging as promising candidates for advanced applications in chiral materials, optoelectronics, and molecular electronics. In this review, we proposed a concise and systematic classification of multiple helicenes into linear, cyclic, and cross-linked types, offering a structural framework to better understand their growing diversity. Based on this classification, we have systematically summarized the research progress in the synthesis methods of multiple helicenes with different stereo structures reported in recent years.

Looking ahead, the development of more general, modular, and stereoselective synthetic strategies will be crucial for accessing a broad range of multiple helicenes with various topologies and properties. In addition, a deeper understanding of relationships between structure and property, particularly how the topology influences chiroptical, electronic, and photophysical behaviours, will be essential for rational molecular design. Furthermore, the integration of multiple helicenes into functional devices and supramolecular systems holds great promise for the development of advanced chiral materials.

We hope that this review will draw greater attention to the class of multiple helicenes and provide valuable guidance for their design and synthesis, thereby facilitating the development of novel molecules with diverse and unique properties and ultimately advancing not only the field of multiple helicenes but also the whole helicene chemistry.

Conflicts of interest

There are no conflicts to declare.

Data availability

No supporting data are included in this article.

Acknowledgements

We thank the National Natural Science Foundation of China (92256304) and the Ministry of Science and Technology of China (2022YFA1204401) for financial support.

References

1 Y. Shen and C.-F. Chen, *Chem. Rev.*, 2012, **112**, 1463–1535.
2 M. Gingras, *Chem. Soc. Rev.*, 2013, **42**, 968–1006.
3 M. Gingras, *Chem. Soc. Rev.*, 2013, **42**, 1051–1095.
4 W.-B. Lin, M. Li, L. Fang and C.-F. Chen, *Chin. Chem. Lett.*, 2018, **29**, 40–46.
5 R. Hassey, E. J. Swain, N. I. Hammer, D. Venkataraman and M. D. Barnes, *Science*, 2006, **314**, 1437–1439.
6 W.-L. Zhao, M. Li, H.-Y. Lu and C.-F. Chen, *Chem. Commun.*, 2019, **55**, 13793–13803.
7 R. R. Gataullin, *Russ. J. Org. Chem.*, 2019, **55**, 1247–1274.
8 K. Dhbaibi, L. Favereau and J. Crassous, *Chem. Rev.*, 2019, **119**, 8846–8953.
9 W.-C. Guo, W.-L. Zhao, K.-K. Tan, M. Li and C.-F. Chen, *Angew. Chem., Int. Ed.*, 2024, **63**, e202401835.
10 M. Li, Y.-F. Wang, D.-W. Zhang, D. Zhang, Z.-Q. Hu, L. Duan and C.-F. Chen, *Sci. China Mater.*, 2021, **64**, 899–908.
11 D.-C. Yang, M. Li and C.-F. Chen, *Chem. Commun.*, 2017, **53**, 9336–9339.
12 E. Clar, C. T. Ironside and M. Zander, *J. Chem. Soc.*, 1959, 142–147.
13 T. Mori, *Chem. Rev.*, 2021, **121**, 2373–2412.
14 A. Tsurusaki and K. Kamikawa, *Chem. Lett.*, 2021, **50**, 1913–1932.
15 Y.-F. Wu, L. Zhang, Q. Zhang, S.-Y. Xie and L.-S. Zheng, *Org. Chem. Front.*, 2022, **9**, 4726–4743.
16 M. Satoh, Y. Shibata and K. Tanaka, *Chem. – Eur. J.*, 2018, **24**, 5434–5438.
17 Y. Kimura, Y. Shibata, K. Noguchi and K. Tanaka, *Eur. J. Org. Chem.*, 2019, 1390–1396.
18 S. Kinoshita, R. Yamano, Y. Shibata, Y. Tanaka, K. Hanada, T. Matsumoto, K. Miyamoto, A. Muranaka, M. Uchiyama and K. Tanaka, *Angew. Chem., Int. Ed.*, 2020, **59**, 11020–11027.
19 K. Hanada, J. Nogami, K. Miyamoto, N. Hayase, Y. Nagashima, Y. Tanaka, A. Muranaka, M. Uchiyama and K. Tanaka, *Chem. – Eur. J.*, 2021, **27**, 9313–9319.
20 Q. Jiang, Y. Han, Y. Zou, H. Phan, L. Yuan, T. S. Herng, J. Ding and C. Chi, *Chem. – Eur. J.*, 2020, **26**, 15613–15622.
21 J. M. dos Santos, D. Sun, J. M. Moreno-Naranjo, D. Hall, F. Zinna, S. T. J. Ryan, W. Shi, T. Matulaitis, D. B. Cordes, A. M. Z. Slawin, D. Beljonne, S. L. Warriner, Y. Olivier, M. J. Fuchter and E. Zysman-Colman, *J. Mater. Chem. C*, 2022, **10**, 4861–4870.
22 W. Yang, N. Li, J. Miao, L. Zhan, S. Gong, Z. Huang and C. Yang, *CCS Chem.*, 2022, **4**, 3463–3471.
23 X. Xiao, S. K. Pedersen, D. Aranda, J. Yang, R. A. Wiscons, M. Pittelkow, M. L. Steigerwald, F. Santoro, N. J. Schuster and C. Nuckolls, *J. Am. Chem. Soc.*, 2021, **143**, 983–991.
24 J. Dong, L. Chen, Q. Feng and D.-T. Yang, *Angew. Chem., Int. Ed.*, 2025, **64**, e202417200.
25 F. Chen, T. Tanaka, Y. S. Hong, T. Mori, D. Kim and A. Osuka, *Angew. Chem., Int. Ed.*, 2017, **56**, 14688–14693.

26 A. Robert, P. Dechambenoit, E. A. Hillard, H. Bock and F. Durola, *Chem. Commun.*, 2017, **53**, 11540–11543.
27 C. Qu, Y. Xu, Y. Wang, Y. Nie, K. Ye, H. Zhang and Z. Zhang, *Angew. Chem., Int. Ed.*, 2024, **63**, e202400661.
28 Z. Sun, C. Yi, Q. Liang, C. Bingi, W. Zhu, P. Qiang, D. Wu and F. Zhang, *Org. Lett.*, 2020, **22**, 209–213.
29 M. Yang, I. S. Park and T. Yasuda, *J. Am. Chem. Soc.*, 2020, **142**, 19468–19472.
30 J.-K. Li, X.-Y. Chen, Y.-L. Guo, X.-C. Wang, A. C.-H. Sue, X.-Y. Cao and X.-Y. Wang, *J. Am. Chem. Soc.*, 2021, **143**, 17958–17963.
31 G. Meng, J. Zhou, X.-S. Han, W. Zhao, Y. Zhang, M. Li, C.-F. Chen, D. Zhang and L. Duan, *Adv. Mater.*, 2024, **36**, 2307420.
32 Y.-Y. Ju, L.-E. Xie, J.-F. Xing, Q.-S. Deng, X.-W. Chen, L.-X. Huang, G.-H. Nie, Y.-Z. Tan and B. Zhang, *Angew. Chem., Int. Ed.*, 2025, **64**, e202414383.
33 Y. Hu, G. M. Paternò, X.-Y. Wang, X.-C. Wang, M. Guizzardi, Q. Chen, D. Schollmeyer, X.-Y. Cao, G. Cerullo, F. Scotognella, K. Müllen and A. Narita, *J. Am. Chem. Soc.*, 2019, **141**, 12797–12803.
34 H. Chang, H. Liu, E. Dmitrieva, Q. Chen, J. Ma, P. He, P. Liu, A. A. Popov, X.-Y. Cao, X.-Y. Wang, Y. Zou, A. Narita, K. Müllen, H. Peng and Y. Hu, *Chem. Commun.*, 2020, **56**, 15181–15184.
35 Y. Liu, L. Yuan, Z. Fan, J. Yang, Y. Wang and C. Dou, *Chem. Sci.*, 2024, **15**, 12819–12826.
36 C. Zeng, C. Xiao, X. Feng, L. Zhang, W. Jiang and Z. Wang, *Angew. Chem., Int. Ed.*, 2018, **57**, 10933–10937.
37 L. Zhang, I. Song, J. Ahn, M. Han, M. Linares, M. Surin, H.-J. Zhang, J. H. Oh and J. Lin, *Nat. Commun.*, 2021, **12**, 142.
38 J. Wang, C. Shen, G. Zhang, F. Gan, Y. Ding and H. Qiu, *Angew. Chem., Int. Ed.*, 2022, **61**, e202115979.
39 J.-K. Li, X.-Y. Chen, W.-L. Zhao, Y.-L. Guo, Y. Zhang, X.-C. Wang, A. C.-H. Sue, X.-Y. Cao, M. Li, C.-F. Chen and X.-Y. Wang, *Angew. Chem., Int. Ed.*, 2023, **62**, e202215367.
40 H. Saito, A. Uchida and S. Watanabe, *J. Org. Chem.*, 2017, **82**, 5663–5668.
41 K. Kawai, K. Kato, L. Peng, Y. Segawa, L. T. Scott and K. Itami, *Org. Lett.*, 2018, **20**, 1932–1935.
42 Y. Chen, R. Zhou, X. Liu, C. Yang, T. Wang, F. Shi and L. Zhang, *Chem. Commun.*, 2022, **58**, 4671–4674.
43 Y. Liang, S. Wang, M. Tang, L. Wu, L. Bian, L. Jiang, Z.-B. Tang, J. Liu, A. Guan and Z. Liu, *Angew. Chem., Int. Ed.*, 2023, **62**, e202218839.
44 F. Zhou, Z. Huang, Z. Huang, R. Cheng, Y. Yang and J. You, *Org. Lett.*, 2021, **23**, 4559–4563.
45 J. Liu, L. Jiang, H. Chang, H. Liu, X.-Y. Cao, Y. Zou and Y. Hu, *Chem. Commun.*, 2022, **58**, 13087–13090.
46 W. Xu, J. Wei, K. Tang, Z. Ma, J. Shi, C. Li and H. Wang, *Org. Chem. Front.*, 2022, **9**, 5578–5585.
47 K. Kato, Y. Segawa, L. T. Scott and K. Itami, *Angew. Chem., Int. Ed.*, 2018, **57**, 1337–1341.
48 D. Meng, G. Liu, C. Xiao, Y. Shi, L. Zhang, L. Jiang, K. K. Baldridge, Y. Li, J. S. Siegel and Z. Wang, *J. Am. Chem. Soc.*, 2019, **141**, 5402–5408.
49 K. Zhang, Z.-C. Chen, Y.-F. Wu, H.-R. Tian, L. Zhang, M.-L. Zhang, S.-L. Deng, Q. Zhang, S.-Y. Xie and L.-S. Zheng, *Angew. Chem., Int. Ed.*, 2025, **64**, e202417269.
50 Y.-F. Wu, S.-W. Ying, L.-Y. Su, J.-J. Du, L. Zhang, B.-W. Chen, H.-R. Tian, H. Xu, M.-L. Zhang, X. Yan, Q. Zhang, S.-Y. Xie and L.-S. Zheng, *J. Am. Chem. Soc.*, 2022, **144**, 10736–10742.
51 Y.-F. Wu, S.-W. Ying, S.-D. Liao, L. Zhang, J.-J. Du, B.-W. Chen, H.-R. Tian, F.-F. Xie, H. Xu, S.-L. Deng, Q. Zhang, S.-Y. Xie and L.-S. Zheng, *Angew. Chem., Int. Ed.*, 2022, **61**, e202204334.
52 Y. Zhu, Z. Xia, Z. Cai, Z. Yuan, N. Jiang, T. Li, Y. Wang, X. Guo, Z. Li, S. Ma, D. Zhong, Y. Li and J. Wang, *J. Am. Chem. Soc.*, 2018, **140**, 4222–4226.
53 Y. Wang, Z. Yin, Y. Zhu, J. Gu, Y. Li and J. Wang, *Angew. Chem., Int. Ed.*, 2019, **58**, 587–591.
54 X. Guo, Z. Yuan, Y. Zhu, Z. Li, R. Huang, Z. Xia, W. Zhang, Y. Li and J. Wang, *Angew. Chem., Int. Ed.*, 2019, **58**, 16966–16972.
55 Y. Zhu, X. Guo, Y. Li and J. Wang, *J. Am. Chem. Soc.*, 2019, **141**, 5511–5517.